RESEARCH ARTICLE

WILEY

Structure-preserving space-time discretization of large-strain thermo-viscoelasticity in the framework of GENERIC

Mark Schiebl | **Peter Betsch**

Institute of Mechanics, Karlsruhe Institute of Technology, Karlsruhe, Germany

Correspondence
Peter Betsch, Institute of Mechanics, Karlsruhe Institute of Technology, 76131 Karlsruhe, Germany.
Email: peter.betsch@kit.edu

Funding information
Deutsche Forschungsgemeinschaft, Grant/Award Number: 388118188 (BE 2285/13-1)

Abstract

Large-strain thermo-viscoelasticity is described in the framework of GENERIC. To this end, a new material representation of the inelastic part of the dissipative bracket is proposed. The bracket form of GENERIC generates the governing equations for large-strain thermo-viscoelasticity including the nonlinear evolution law for the internal variables associated with inelastic deformations. The GENERIC formalism facilitates the free choice of the thermodynamic variable. In particular, one may choose (i) the internal energy density, (ii) the entropy density, or (iii) the absolute temperature as the thermodynamic variable. A mixed finite element method is proposed for the discretization in space which preserves the GENERIC form of the resulting semi-discrete evolution equations. The GENERIC-consistent space discretization makes possible the design of structure-preserving time-stepping schemes. The mid-point type discretization in time yields three alternative schemes. Depending on the specific choice of the thermodynamic variable, these schemes are shown to be partially structure-preserving. In addition to that, it is shown that a slight modification of the mid-point type schemes yields fully structure-preserving schemes. In particular, three alternative energy-momentum-entropy consistent schemes are devised associated with the specific choice of the thermodynamic variable. Numerical investigations are presented which confirm the theoretical findings and shed light on the numerical stability of the newly developed schemes.

KEYWORDS

energy-momentum-entropy schemes, structure-preserving numerical methods, thermo-mechanically coupled problems

1 | INTRODUCTION

Structure-preserving time integration schemes, also known as geometric integrators, have been an active topic of research in applied mathematics and computational mechanics for decades (see Leimkuhler and Reich[1] and Hairer et al.[2] for a large number of contributions to the field). Geometric integrators are designed in such a way, that the numerical

method respects the fundamental physics of the problem by preserving the geometric properties in a discrete setting. Associated with the preservation of the geometric structure excellent long-term performance and numerical stability have been reported. In the realm of Langragian/Hamiltonian mechanics, many geometric integrators can be gathered around two classes: Variational integrators (see, e.g., Marsden and Ratiu,[3] Lew et al.,[4] and Lall and West[5] for more details) and energy-momentum integrators (see, e.g., LaBudde and Greenspan,[6,7] Gonzalez,[8] or Betsch[9] for a comprehensive overview of previous developments), and energy-decaying variants thereof; see Gebhardt et al.[10] and references therein.

Numerous attempts have been made to extend structure-preserving schemes to the domain of non-conservative mechanical systems, such as port-Hamiltonian systems,[11] viscoelasticity,[12,13] elastoplasticity,[14] and thermo-viscoelasticity.[15-17] Unlike the Lagrangian/Hamiltonian case, these structure-preserving schemes do not emerge from an unifying theory.

However, the GENERIC (General Equation for Non-Equilibrium Reversible-Irreversible Coupling) provides a double-generator framework which expresses thermomechanical models of dissipative materials (or generalized standard materials) in a unifying formalism. Its formulation is based on an additive decomposition of the time-evolution equations into a reversible part and a dissipative part and can be seen as a natural extension of Hamiltonian mechanics to the dissipative regime (see, e.g., Badlyan et al.[18] for a relation to Port-Hamiltonian systems). Originally, the GENERIC framework has been developed in the context of complex fluids[19,20] (see Öttinger[21] for a comprehensive account of the GENERIC formalism).

An early application of the GENERIC formalism to finite strain thermo-elasticity is due to Hütter and Tervoort,[22] albeit in a Eulerian setting which is quite uncommon in solid mechanics. Later the Lagrangian setting has been used in References 23-25 to develop the GENERIC framework for non-isothermal solid mechanics. Moreover, Hütter and Svendsen[23,24] prefer to use the absolute temperature as thermodynamic state variable, while in Mielke[25] a special form of GENERIC is devised which makes possible the free choice of the thermodynamic variable.

In the field of computational solid mechanics Romero[26] was the first who recognized the great potential of the GENERIC framework for the design of structure-preserving time-stepping schemes. Since the GENERIC framework automatically ensures the thermodynamic admissibility of the time-evolution equations, it provides an ideal starting point for the development of thermodynamically consistent (TC) integrators. In particular, TC integrators comply with both the first and second law of thermodynamics, independent of the size of the time-step. Therefore, TC integrators may also be termed "energy-entropy" integrators. If TC integrators further respect symmetries of the underlying mechanical system, they can be viewed as extension to the dissipative regime of energy-momentum (EM) integrators previously developed for Hamiltonian systems with symmetry; see, for example, References 8,27,28.

Consequently, GENERIC provides a solid theoretical foundation for the design of energy-momentum-entropy (EME) methods, as shown, for example, in References 29-32 for entropy-based and in References 33-36 for temperature-based formulations.

The construction of GENERIC-based structure-preserving numerical methods is not limited to EME methods. For example, the so-called GENERIC integrators have been developed in References 37 and 38, which can be regarded as extension of symplectic integrators for Hamiltonian systems to the realm of dissipative systems. Another example are GENERIC-based structure-preserving numerical methods for neural networks.[18]

Considering the description of large strain thermoelasticity, a GENERIC-based weak form is derived in Betsch and Schiebl[39] which makes possible the free choice of thermodynamic state variable following the approach presented in Mielke.[25] It was shown in Betsch and Schiebl[39] that application of the standard mid-point rule to the GENERIC-based weak form already yields partially structure-preserving schemes. For example, choosing the internal energy density as thermodynamic variable leads to an EM scheme, while the choice of entropy density yields a momentum-entropy method.

However, despite of their (partially) structure-preserving properties, all of the mid-point type schemes considered in Betsch and Schiebl[39] cannot prevent numerical instabilities. This issue was resolved in Betsch and Schiebl[40] by resorting to a GENERIC-consistent space discretization followed by the application of partitioned discrete derivatives in the sense of Gonzalez.[41] The resulting EME schemes satisfy a specific Lyapunov-type stability estimate and thus do not exhibit any numerical instabilities.

The main goal of the present work is to extend our previous work[39,40] to the realm of thermo-viscoelasticity. In particular, we aim at a material formulation of isotropic large strain thermo-viscoelasticity which makes possible the free choice of thermodynamic state variable. To this end, we build on previous work by Hütter and Svendsen[24] who laid the theoretical basis for the GENERIC description of thermo-viscoelasticity.

The rest of this article is organized as follows. In Section 2, the bracket form of the GENERIC formalism is introduced for thermo-viscoelasticity with heat conduction. In particular, in Section 3, a new material version of the inelastic dissipative bracket is proposed, which makes possible the free choice of the thermodynamic variable. In Section 4, a mixed finite element approach is proposed which yields a GENERIC-consistent semi-discrete form of the evolution equations. The mid-point type discretization in time is dealt with in Section 5 leading to alternative (partially) structure-preserving schemes. After the numerical investigations in Section 6, conclusions are drawn in Section 7.

2 | GENERIC-BASED FORMULATION OF LARGE STRAIN THERMO-VISCOELASTICITY

The present work relies on a material description of large strain thermo-viscoelasticity within the framework of GENERIC. The developments presented herein extend our previous work[39] on thermo-elasticity to the realm of inelastic deformations. For more background on the GENERIC framework the reader is referred to Betsch and Schiebl[39] and the references therein. In the GENERIC framework, the time-evolution of any functional $\mathcal{A}$ is governed by

$$\frac{d\mathcal{A}}{dt} = \{\mathcal{A}, \mathcal{E}\} + [\mathcal{A}, \mathcal{S}]. \tag{1}$$

The evolution equation (1) is valid for closed systems in which the boundaries are disregarded. We consider a continuum body with material points $\mathbf{X} = X^A \mathbf{e}_A$ in the reference configuration $\mathcal{B} \subset \mathbb{R}^3$ (Figure 1). The material coordinates X^A refer to canonical base vectors $\mathbf{e}_A \in \mathbb{R}^3$. Here and in the sequel, the summation convention applies to repeated indices. Within the Lagrangian description of continuum mechanics the deformed configuration of the body at time t is characterized by the deformation map $\boldsymbol{\varphi} : \mathcal{B} \times \mathcal{I} \mapsto \mathbb{R}^3$, where $\mathcal{I} = [0, T]$ is the time interval of interest. Accordingly, the placement at time t of the material point $\mathbf{X} \in \mathcal{B}$ is given by $\mathbf{x} = \boldsymbol{\varphi}(\mathbf{X}, t)$. The corresponding velocity field $\mathbf{v} : \mathcal{B} \times \mathcal{I} \mapsto \mathbb{R}^3$ is defined by $\mathbf{v} = \dot{\boldsymbol{\varphi}}$, where a superposed dot denotes the material time derivative. The deformation gradient is given by

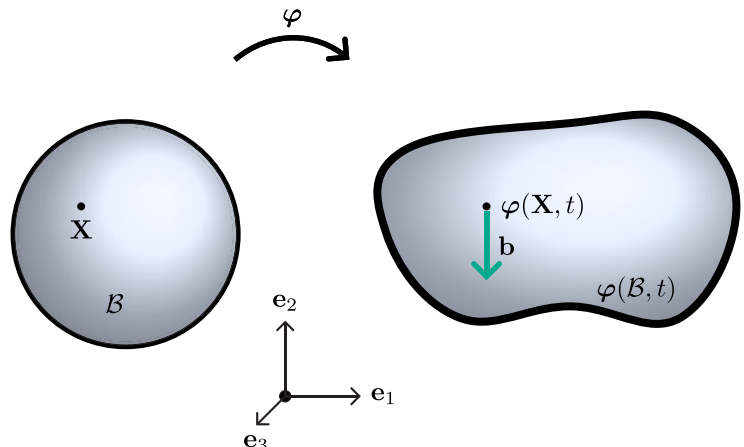$$\mathbf{F} = \partial_{\mathbf{X}} \boldsymbol{\varphi}, \tag{2}$$

or, in components, $(\mathbf{F})^{i}_{.A} = \partial x^i / \partial X^A$. Furthermore, the right Cauchy-Green tensor reads

$$\mathbf{C} = \mathbf{F}^{\mathrm{T}} \mathbf{F}. \tag{3}$$

In the GENERIC (1), we consider functionals of the form

$$\mathcal{A} = \mathcal{A}(\boldsymbol{\varphi}, \mathbf{p}, \tau, \mathbf{C}_p^{-1}) = \int_{\mathcal{B}} a(\boldsymbol{\varphi}, \mathbf{F}, \mathbf{p}, \tau, \mathbf{C}_p^{-1}) \, dV, \tag{4}$$

where $\mathbf{p} = \rho \mathbf{v}$ is the linear momentum density and $\rho : \mathcal{B} \mapsto \mathbb{R}_+$ is the mass density in the reference configuration. Moreover, $\tau : \mathcal{B} \times \mathcal{I} \mapsto \mathbb{R}$ is a generalized thermodynamic field which may be chosen from among three alternatives,

FIGURE 1 Reference configuration $\mathcal{B}$ and deformed configuration $\boldsymbol{\varphi}(\mathcal{B}, t)$ at time t. For now the focus is on the motion of isolated thermomechanically coupled solids. That is, external tractions acting on the boundary as well heat fluxes across the boundary are disregarded

$\tau \in \{\theta, \eta, u\}$. The three alternative fields are the absolute temperature θ, the entropy density η, and the internal energy density u.

To describe inelastic deformations, we make use of the internal variable $\mathbf{C}_p^{-1} : \mathcal{B} \times \mathcal{I} \mapsto \mathbb{R}^{3 \times 3}$. Since we focus on isotropic inelastic deformations, $\mathbf{C}_p^{-1}$ is assumed to be symmetric, that is, $(\mathbf{C}_p^{-1})^{\mathrm{T}} = \mathbf{C}_p^{-1}$. Therefore the density function a in (4) is subject to the same isotropic restrictions as the Helmholtz free energy function, to be introduced in Section 3.

GENERIC (1) decouples reversible and irreversible processes. In particular, the Poisson bracket $\{\cdot, \cdot\}$ is responsible for reversible processes, while the dissipative (or friction) bracket $[\cdot, \cdot]$ embodies irreversible processes. Accordingly, these two brackets constitute fundamental entities of the GENERIC framework and shall be specified next. Since inelastic deformations are purely irreversible, the Poisson bracket retains its thermo-elastic form (see Betsch and Schiebl[39])

$$\{\mathcal{A}, \mathcal{B}\} = \int_{\mathcal{B}} \left(\delta_{\varphi} a + \mathrm{Div} \left(\frac{\delta_{\tau} a}{\partial_{\tau \eta}} \partial_{\mathbf{F}} \eta \right) \right) \cdot \delta_{\mathbf{p}} b - \left(\delta_{\varphi} b + \mathrm{Div} \left(\frac{\delta_{\tau} b}{\partial_{\tau \eta}} \partial_{\mathbf{F}} \eta \right) \right) \cdot \delta_{\mathbf{p}} a \ \mathrm{d}V, \tag{5}$$

where $\mathcal{A}$ and $\mathcal{B}$ are arbitrary functionals of the form (4). Furthermore, the functional derivatives in (5) are given by

$$\delta_{\varphi} a = \partial_{\varphi} a - \mathrm{Div} \partial_{\mathbf{F}} a,$$
$$\delta_{\mathbf{p}} a = \partial_{\mathbf{p}} a,$$
$$\delta_{\tau} a = \partial_{\tau} a,$$
$$\delta_{\mathbf{C}_p^{-1}} a = \partial_{\mathbf{C}_p^{-1}} a. \tag{6}$$

In (5), η denotes the entropy density giving rise to the total entropy of the system

$$S(\varphi, \tau, \mathbf{C}_p^{-1}) = \int_{\mathcal{B}} \eta(\mathbf{F}, \tau, \mathbf{C}_p^{-1}) \ \mathrm{d}V. \tag{7}$$

The dissipative bracket for the thermo-viscoelastic problem at hand can be additively decomposed into a part due to heat conduction and a part taking into account inelastic deformations:

$$[\mathcal{A}, \mathcal{B}] = [\mathcal{A}, \mathcal{B}]_{\mathrm{cond}} + [\mathcal{A}, \mathcal{B}]_{\mathrm{inel}}. \tag{8}$$

In analogy to thermo-elasticity with heat conduction, the dissipative bracket accounting for heat conduction is given by (see Betsch and Schiebl[39])

$$[\mathcal{A}, \mathcal{B}]_{\mathrm{cond}} = \int_{\mathcal{B}} \nabla \left(\frac{\delta_{\tau} a}{\partial_{\tau} u} \right) \cdot \Theta^2 \mathbf{K} \nabla \left(\frac{\delta_{\tau} b}{\partial_{\tau} u} \right) \ \mathrm{d}V. \tag{9}$$

Here, $\mathbf{K} = \mathbf{K}(\mathbf{C}, \tau)$ is the material conductivity tensor, for which we assume that $\mathbf{K}^{\mathrm{T}} = \mathbf{K}$ and $\mathbf{a} : \mathbf{K} : \mathbf{a} \geq 0$ holds for all $\mathbf{a} \in \mathbb{R}^3$. An important element of the GENERIC framework is that the absolute temperature takes the form

$$\Theta(\mathbf{F}, \tau, \mathbf{C}_p^{-1}) = \frac{\partial_{\tau} u(\mathbf{F}, \tau, \mathbf{C}_p^{-1})}{\partial_{\tau \eta}(\mathbf{F}, \tau, \mathbf{C}_p^{-1})}. \tag{10}$$

In (9) and (10), u denotes the internal energy density which, together with the kinetic energy and the potential of dead loads, constitutes the total energy of the system

$$\mathcal{E}(\varphi, \mathbf{p}, \tau, \mathbf{C}_p^{-1}) = \int_{\mathcal{B}} \left(\frac{1}{2} \rho^{-1} \mathbf{p} \cdot \mathbf{p} + u(\mathbf{F}, \tau, \mathbf{C}_p^{-1}) - \mathbf{b} \cdot \varphi \right) \ \mathrm{d}V. \tag{11}$$

Here, $\mathbf{b} : \mathcal{B} \mapsto \mathbb{R}^3$ represent prescribed body forces which, for simplicity, are assumed to be dead loads.

Concerning the contribution of inelastic deformations, we introduce the following form of the dissipative bracket (see Section 3 for further details):

$$[\mathcal{A}, \mathcal{B}]_{\mathrm{inel}} = \int_{\mathcal{B}} 2 \left(\frac{\delta_{\tau} a}{\partial_{\tau} u} \partial_{\mathbf{C}_p^{-1}} u \mathbf{C}_p^{-1} - \delta_{\mathbf{C}_p^{-1}} a \mathbf{C}_p^{-1} \right) : \Theta \mathcal{N} : 2 \left(\frac{\delta_{\tau} b}{\partial_{\tau} u} \partial_{\mathbf{C}_p^{-1}} u \mathbf{C}_p^{-1} - \delta_{\mathbf{C}_p^{-1}} b \mathbf{C}_p^{-1} \right) \ \mathrm{d}V. \tag{12}$$

The fourth-order inelastic material flow tensor $\mathcal{N}$ has the properties $\mathcal{N}^{\mathrm{T}} = \mathcal{N}$ (major symmetry) and $\mathbf{M} : \mathcal{N} : \mathbf{M} \geq 0$ (positive semi-definiteness) for all $\mathbf{M}$ given in (17).

It can be easily verified that the Poisson bracket (5) is skew-symmetric ($\{\mathcal{A}, \mathcal{B}\} = -\{\mathcal{B}, \mathcal{A}\}$), the dissipative bracket (12) is symmetric ($[\mathcal{A}, \mathcal{B}] = [\mathcal{B}, \mathcal{A}]$) and further satisfies the non-negativity condition $[\mathcal{A}, \mathcal{A}] \geq 0$. Moreover, the two brackets satisfy the fundamental degeneracy (or non-interaction) conditions $\{\mathcal{A}, \mathcal{S}\} = 0$ and $[\mathcal{A}, \mathcal{E}] = 0$. In conjunction with these properties of the two brackets, GENERIC (1) ensures for closed systems (i) the conservation of total energy ($\mathrm{d}\mathcal{E}/\mathrm{d}t = 0$), and (ii) a non-decreasing total entropy ($\mathrm{d}\mathcal{S}/\mathrm{d}t \geq 0$). Due to these structural properties, the GENERIC-based formulation offers an ideal starting point for the design of structure-preserving numerical methods.

2.1 | Local evolution equations

We provide a short outline of the local evolution equations emanating from GENERIC (1). With regard to (1) the total energy $\mathcal{E}$ generates the reversible contribution through the Poisson bracket $\{\mathcal{A}, \mathcal{E}\}$. Using expression (11) for the total energy along with formulas (6) for the variational derivatives, Poisson bracket (5) yields

$$\{\mathcal{A}, \mathcal{E}\} = \int_{\mathcal{B}} \left(\delta_{\varphi} a + \mathrm{Div} \left(\frac{\delta_{\tau} a}{\partial_{\tau} \eta} \partial_{\mathbf{F}} \eta \right) \right) \cdot \rho^{-1} \mathbf{p} + (\mathbf{b} + \mathrm{Div}\mathbf{P}) \cdot \delta_{\mathbf{p}} a \, \mathrm{d}V, \tag{13}$$

where the first Piola-Kirchhoff stress tensor $\mathbf{P} = \mathbf{P}(\mathbf{F}, \tau, \mathbf{C}_p^{-1})$ takes the form

$$\mathbf{P} = \partial_{\mathbf{F}} u - \Theta \partial_{\mathbf{F}} \eta. \tag{14}$$

The irreversible contribution to GENERIC (1) is generated by the total entropy $\mathcal{S}$ through the dissipative bracket $[\mathcal{A}, \mathcal{S}]$. Inserting expression (7) for the total entropy into the dissipative bracket (8) leads to

$$[\mathcal{A}, \mathcal{S}] = \int_{\mathcal{B}} \nabla \left(\frac{\delta_{\tau} a}{\partial_{\tau} u} \right) \cdot \mathbf{Q} \, \mathrm{d}V + \int_{\mathcal{B}} 2 \left(\frac{\delta_{\tau} a}{\partial_{\tau} u} \partial_{\mathbf{C}_p^{-1}} u \mathbf{C}_p^{-1} - \delta_{\mathbf{C}_p^{-1}} a \mathbf{C}_p^{-1} \right) : \mathcal{N} : \mathbf{M} \, \mathrm{d}V, \tag{15}$$

where the material heat flux vector $\mathbf{Q} = \mathbf{Q}(\mathbf{F}, \tau, \mathbf{C}_p^{-1})$ is given by

$$\mathbf{Q} = \Theta^2 \mathbf{K} \nabla \left(\frac{1}{\Theta} \right) = -\mathbf{K} \nabla \Theta \tag{16}$$

and $\mathbf{M} = \mathbf{M}(\mathbf{F}, \tau, \mathbf{C}_p^{-1})$ denotes the material representation of the Mandel stress tensor, which takes the form

$$\mathbf{M} = 2 \left(\partial_{\mathbf{C}_p^{-1}} u - \Theta \partial_{\mathbf{C}_p^{-1}} \eta \right) \mathbf{C}_p^{-1}. \tag{17}$$

It is important to realize that in (14), (16) and (17), Θ is the temperature field which has been introduced in (10). These relationships are representative for the GENERIC-based formulation.

With regard to the left-hand side of GENERIC (1) and expression (4) for functional $\mathcal{A}$, the time derivative of $\mathcal{A}$ can be written as

$$\frac{\mathrm{d}}{\mathrm{d}t} \mathcal{A} = \int_{\mathcal{B}} \left(\delta_{\varphi} a \cdot \dot{\varphi} + \delta_{\mathbf{p}} a \cdot \dot{\mathbf{p}} + \delta_{\tau} a \dot{\tau} + \delta_{\mathbf{C}_p^{-1}} a : \overline{\dot{\mathbf{C}}_p^{-1}} \right) \, \mathrm{d}V. \tag{18}$$

In the last equation $\overline{\dot{\mathbf{C}}_p^{-1}}$ stands for $\partial \mathbf{C}_p^{-1}/\partial t$. Substituting (18), (13), and (15) into GENERIC (1), we arrive at

$$0 = \int_{\mathcal{B}} \delta_{\varphi} a \cdot \left(\dot{\varphi} - \rho^{-1} \mathbf{p} \right) \, \mathrm{d}V$$

$$+ \int_{\mathcal{B}} \delta_{\mathbf{p}} a \cdot (\dot{\mathbf{p}} - (\mathbf{b} + \mathrm{Div}\mathbf{P})) \, \mathrm{d}V$$

$$+ \int_{\mathcal{B}} \delta_{\tau} a \left(\dot{\tau} - \frac{2}{\partial_{\tau} u} \left(\partial_{\mathbf{C}_p^{-1}} u \mathbf{C}_p^{-1} \right) : \mathcal{N} : \mathbf{M} \right) - \mathrm{Div} \left(\frac{\delta_{\tau} a}{\partial_{\tau} \eta} \partial_{\mathbf{F}} \eta \right) \cdot \rho^{-1} \mathbf{p} - \nabla \left(\frac{\delta_{\tau} a}{\partial_{\tau} u} \right) \cdot \mathbf{Q} \, \mathrm{d}V$$

$$+ \int_{\mathcal{B}} \delta_{\mathbf{C}_p^{-1}} a : \left(\overline{\dot{\mathbf{C}}_p^{-1}} + 2 \left[\mathcal{N} : \mathbf{M} \right] \mathbf{C}_p^{-1} \right) \, \mathrm{d}V. \tag{19}$$

This equation has to hold for arbitrary functionals $\mathcal{A}$ of the form (4). Standard arguments now lead to the local evolution equations emanating from GENERIC (1):

$$\dot{\boldsymbol{\varphi}} = \rho^{-1}\mathbf{p},$$

$$\dot{\mathbf{p}} = \mathbf{b} + \mathrm{Div}\mathbf{P},$$

$$\dot{\tau} = \frac{2}{\partial_\tau u}\left(\partial_{\mathbf{C}_p^{-1}}u\mathbf{C}_p^{-1}\right) : \mathcal{N} : \mathbf{M} - \frac{1}{\partial_{\tau\eta}}\partial_{\mathbf{F}}\eta : \nabla(\rho^{-1}\mathbf{p}) - \frac{1}{\partial_\tau u}\mathrm{Div}\mathbf{Q},$$

$$\dot{\overline{\mathbf{C}_p^{-1}}} = -2\left(\mathcal{N} : \mathbf{M}\right)\mathbf{C}_p^{-1}. \tag{20}$$

We stress again that in the above formulas the first Piola-Kirchhoff stress tensor $\mathbf{P}$, the Mandel stress tensor $\mathbf{M}$ and the heat flux vector $\mathbf{Q}$ are given by formulas (14), (17), and (16), respectively.

2.2 | GENERIC-based weak form of the IBVP

Starting from the GENERIC-based local evolution equations (20), we deduce the weak form of the initial boundary value problem (IBVP) pertaining to finite-strain thermo-viscoelasticity. To this end, we decompose the boundary $\partial\mathcal{B}$ of the continuum body into a displacement boundary $\partial_\varphi\mathcal{B}$, on which $\boldsymbol{\varphi} = \overline{\boldsymbol{\varphi}}$, and a traction boundary $\partial_\sigma\mathcal{B}$, on which $\mathbf{PN} = \bar{\mathbf{t}}$, where $\overline{\boldsymbol{\varphi}}$ and $\bar{\mathbf{t}}$ are prescribed functions for $t \geq 0$ (Figure 2). Moreover, $\partial_\varphi\mathcal{B} \cup \partial_\sigma\mathcal{B} = \partial\mathcal{B}$ and $\partial_\varphi\mathcal{B} \cap \partial_\sigma\mathcal{B} = \emptyset$. Similarly, for the thermal part, we consider the subsets of the boundary $\partial_\tau\mathcal{B}$ and $\partial_q\mathcal{B}$, with the properties $\partial_\tau\mathcal{B} \cup \partial_q\mathcal{B} = \partial\mathcal{B}$ and $\partial_\tau\mathcal{B} \cap \partial_q\mathcal{B} = \emptyset$ (Figure 3). The thermodynamic variable is prescribed on $\partial_\tau\mathcal{B}$, that is, $\tau = \overline{\tau}$, whereas the heat flux is prescribed on $\partial_q\mathcal{B}$, that is, $\mathbf{Q} \cdot \mathbf{N} = \overline{q}$. Both $\overline{\tau}$ and $\overline{q}$ are assumed to be given for $t \geq 0$. We aim at the determination of the motion $\boldsymbol{\varphi} : \mathcal{B} \times \mathcal{I} \mapsto \mathbb{R}^3$, the linear momentum $\mathbf{p} : \mathcal{B} \times \mathcal{I} \mapsto \mathbb{R}^3$, the thermodynamic variable $\tau : \mathcal{B} \times \mathcal{I} \mapsto \mathbb{R}$, and the inelastic deformation $\mathbf{C}_p^{-1} : \mathcal{B} \times \mathcal{I} \mapsto \mathbb{R}^{3\times3}$. The unknown fields are subject to initial conditions of the form $\boldsymbol{\varphi}(\cdot, 0) = \mathbf{X}$, $\mathbf{p}(\cdot, 0) = \rho\mathbf{V}_0$, $\tau(\cdot, 0) = \tau^{\mathrm{ini}}$ and $\mathbf{C}_p^{-1}(\cdot, 0) = \mathbf{I}$ in $\mathcal{B}$. Here, $\mathbf{V}_0$ is a prescribed material velocity field, and τ^{ini} is a prescribed field of the thermodynamic variable $\tau \in \{\theta, \eta, u\}$. The unknown fields are determined by applying a space-time discretization to the weak form of the IBVP at hand.

The weak form of the IBVP can be obtained by scalar multiplying the local evolution Eqs. 20 by suitable test functions and subsequently integrating over domain $\mathcal{B}$. The standard procedure yields

$$0 = \int_{\mathcal{B}} \mathbf{w}_{\boldsymbol{\varphi}} \cdot (\dot{\boldsymbol{\varphi}} - \mathbf{v}) \ \mathrm{d}V$$

$$+ \int_{\mathcal{B}} \left(\mathbf{w_p} \cdot (\rho\dot{\mathbf{v}} - \mathbf{b}) + \mathbf{P} : \nabla\mathbf{w_p}\right) \ \mathrm{d}V - \int_{\partial_\sigma\mathcal{B}} \mathbf{w_p} \cdot \bar{\mathbf{t}} \ \mathrm{d}A$$

$$+ \int_{\mathcal{B}} \mathrm{w}_\tau \left(\dot{\tau} - \frac{2}{\partial_\tau u}\left(\partial_{\mathbf{C}_p^{-1}}u\mathbf{C}_p^{-1}\right) : \mathcal{N} : \mathbf{M} + \frac{1}{\partial_{\tau\eta}}\partial_{\mathbf{F}}\eta : \nabla\mathbf{v}\right) \ \mathrm{d}V$$

$$- \int_{\mathcal{B}} \nabla\left(\frac{\mathrm{w}_\tau}{\partial_\tau u}\right) \cdot \mathbf{Q} \ \mathrm{d}V + \int_{\partial_q\mathcal{B}} \frac{\mathrm{w}_\tau}{\partial_\tau u}\overline{q} \ \mathrm{d}A$$

$$+ \int_{\mathcal{B}} \mathbf{w}_{\mathbf{C}_p^{-1}} : \left(\dot{\overline{\mathbf{C}_p^{-1}}} + 2\left(\mathcal{N} : \mathbf{M}\right)\mathbf{C}_p^{-1}\right) \ \mathrm{d}V, \tag{21}$$
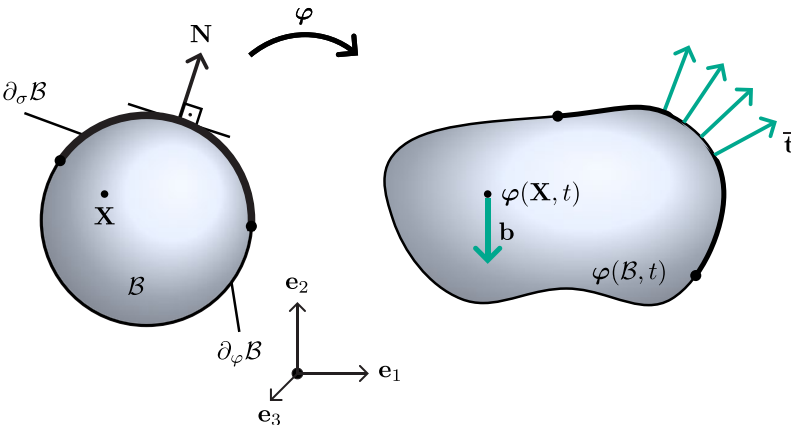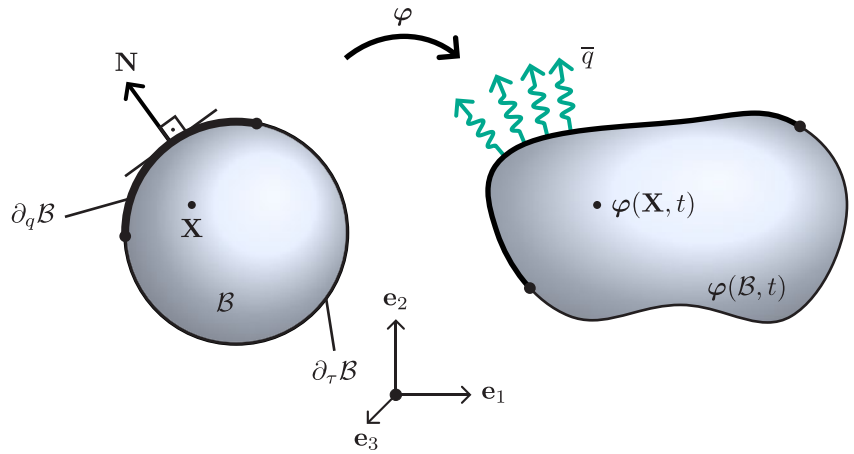

FIGURE 2 Mechanical part of the IBVP. Note that $\bar{\mathbf{t}} = \mathbf{PN}$ denotes prescribed external Piola tractions acting on the current boundary expressed per unit area of the reference boundary $\partial_\sigma\mathcal{B}$

where the velocity field $\mathbf{v} = \rho^{-1}\mathbf{p}$ has been introduced. In weak form (21), $\mathbf{w}_\varphi, \mathbf{w}_\mathbf{p} : \mathcal{B} \mapsto \mathbb{R}^3$, $w_\tau : \mathcal{B} \mapsto \mathbb{R}$ and $\mathbf{w}_{\mathbf{C}_p^{-1}} : \mathcal{B} \mapsto \mathbb{R}^{3\times3}$ are test functions that have to satisfy the boundary conditions $\mathbf{w}_\varphi = \mathbf{0}$ and $\mathbf{w}_\mathbf{p} = \mathbf{0}$ on $\partial_\varphi \mathcal{B}$, and $w_\tau = 0$ on $\partial_\tau \mathcal{B}$.

2.3 | Balance laws

We verify the pertinent balance laws of the IBVP at hand. For that purpose it suffices to consider the pure Neumann problem (i.e., $\partial_\sigma \mathcal{B} = \partial_q \mathcal{B} = \partial \mathcal{B}$). We start with the total linear momentum of the continuum body defined by $\mathbf{L} = \int_\mathcal{B} \mathbf{p} \, dV$. Choosing $(\mathbf{w}_\varphi, \mathbf{w}_\mathbf{p}, w_\tau, \mathbf{w}_{\mathbf{C}_p^{-1}}) = (\mathbf{0}, \boldsymbol{\xi}, 0, \mathbf{0})$, where $\boldsymbol{\xi} \in \mathbb{R}^3$ is arbitrary but constant, weak form (21) leads to

$$\boldsymbol{\xi} \cdot \frac{d\mathbf{L}}{dt} = \boldsymbol{\xi} \cdot \left(\int_\mathcal{B} \mathbf{b} \, dV + \int_{\partial \mathcal{B}} \overline{\mathbf{t}} \, dA \right). \tag{22}$$

Due to the arbitrariness of $\boldsymbol{\xi} \in \mathbb{R}^3$, (22) coincides with the balance law for linear momentum. Note that the parentheses on the right-hand side of (22) contain the resultant external force exerted on the continuum body (see also Figure 2).

The total angular momentum relative to the origin of the inertial frame is defined by $\mathbf{J} = \int_\mathcal{B} \boldsymbol{\varphi} \times \mathbf{p} \, dV$. Choosing $(\mathbf{w}_\varphi, \mathbf{w}_\mathbf{p}, w_\tau, \mathbf{w}_{\mathbf{C}_p^{-1}}) = (\mathbf{p} \times \boldsymbol{\xi}, \boldsymbol{\xi} \times \boldsymbol{\varphi}, 0, \mathbf{0})$, weak form (21) yields

$$\boldsymbol{\xi} \cdot \frac{d\mathbf{J}}{dt} = \boldsymbol{\xi} \cdot \left(\int_\mathcal{B} \boldsymbol{\varphi} \times \mathbf{b} \, dV + \int_{\partial \mathcal{B}} \boldsymbol{\varphi} \times \overline{\mathbf{t}} \, dA \right). \tag{23}$$

Note that the symmetry condition $\mathbf{F}\mathbf{P}^\mathrm{T} = \mathbf{P}\mathbf{F}^\mathrm{T}$ has been employed. Since $\boldsymbol{\xi} \in \mathbb{R}^3$ is arbitrary, (23) corresponds to the balance of angular momentum. The parentheses on the right-hand side of (23) contain the resultant external torque about the origin (see also Figure 2).

Next, we substitute $(\mathbf{w}_\varphi, \mathbf{w}_\mathbf{p}, w_\tau, \mathbf{w}_{\mathbf{C}_p^{-1}}) = (-\mathbf{b}, \rho^{-1}\mathbf{p}, \partial_\tau u, \partial_{\mathbf{C}_p^{-1}} u)$ into weak form (21). A straightforward calculation leads to the balance law for total energy

$$\frac{d}{dt} \int_\mathcal{B} \left(\frac{1}{2} \rho^{-1} \mathbf{p} \cdot \mathbf{p} + u \right) \, dV = \int_\mathcal{B} \mathbf{b} \cdot \dot{\boldsymbol{\varphi}} \, dV + \int_{\partial \mathcal{B}} \left(\rho^{-1} \mathbf{p} \cdot \overline{\mathbf{t}} - \overline{q} \right) \, dA. \tag{24}$$

We choose $(\mathbf{w}_\varphi, \mathbf{w}_\mathbf{p}, w_\tau, \mathbf{w}_{\mathbf{C}_p^{-1}}) = (\mathbf{0}, \rho^{-1}\mathbf{p}, \partial_\tau \eta, \partial_{\mathbf{C}_p^{-1}} \eta)$ concerning the balance of entropy in weak form (21) to obtain

$$
\begin{aligned}
0 &= \int_\mathcal{B} \left(\partial_\mathbf{F} \eta : \dot{\mathbf{F}} + \partial_{\tau\eta} \dot{\tau} + 2\partial_{\mathbf{C}_p^{-1}} \eta : \left((\mathcal{N} : \mathbf{M}) \, \mathbf{C}_p^{-1} \right) - 2 \left(\partial_{\mathbf{C}_p^{-1}} u \mathbf{C}_p^{-1} \right) : \mathcal{N} : \mathbf{M} \right) \, dV \\
&\quad + \int_\mathcal{B} \partial_{\mathbf{C}_p^{-1}} \eta : \overline{\dot{\mathbf{C}_p^{-1}}} - \nabla \left(\frac{\partial_\tau \eta}{\partial_{\tau u}} \right) \cdot \mathbf{Q} \, dV + \int_{\partial \mathcal{B}} \frac{\partial_{\tau\eta}}{\partial_{\tau u}} \overline{q} \, dA \\
&= \int_\mathcal{B} \left(\frac{d\eta}{dt} - \frac{1}{\Theta} \mathbf{M} : \mathcal{N} : \mathbf{M} - \nabla \left(\frac{1}{\Theta} \right) \cdot \Theta^2 \mathbf{K} \nabla \left(\frac{1}{\Theta} \right) \right) \, dV + \int_{\partial \mathcal{B}} \frac{1}{\Theta} \overline{q} \, dA.
\end{aligned}
$$

Here, use has been made of formula (10) for the temperature along with expressions (16) for the material heat flux vector and (17) for the Mandel stress tensor, respectively. The above equation can be rewritten as

$$\frac{\mathrm{d}S}{\mathrm{d}t} + \int_{\partial B} \frac{1}{\Theta} \overline{q} \, \mathrm{d}A = \int_{B} \underbrace{\nabla\left(\frac{1}{\Theta}\right) \cdot \Theta^2 \mathbf{K} \nabla\left(\frac{1}{\Theta}\right)}_{=\mathcal{D}_{\mathrm{cond}} \geq 0} + \underbrace{\frac{1}{\Theta} \mathbf{M} : \mathcal{N} : \mathbf{M}}_{=\mathcal{D}_{\mathrm{inel}} \geq 0} \, \mathrm{d}V \geq 0, \tag{25}$$

where $\mathcal{D}_{\mathrm{inel}}$ is the local production of entropy due to inelastic deformations and $\mathcal{D}_{\mathrm{cond}}$ is the local production of entropy due to heat conduction. The last equation corresponds to the Clausius-Duhem form of the second law of thermodynamics (see, for example, Gonzalez and Stuart,[42] Sec. 5).

3 | INELASTIC PART OF THE DISSIPATIVE BRACKET

The present model for large strain thermo-viscoelasticity relies on the introduction of the internal variable $\mathbf{C}_p^{-1} : B \times \mathcal{I} \mapsto \mathbb{R}^{3\times3}$, whose time-evolution accounts for local inelastic deformations. Following Reese and Govindjee,[43] $\mathbf{C}_p^{-1}$ can be associated with the multiplicative decomposition of the deformation gradient[44]

$$\mathbf{F} = \mathbf{F}_e \mathbf{F}_p \tag{26}$$

into an elastic part $\mathbf{F}_e$ and an inelastic (or viscous) part $\mathbf{F}_p$. Decomposition (26) gives rise to the relationship

$$\mathbf{C}_p = \mathbf{F}_p^{\mathrm{T}} \mathbf{F}_p. \tag{27}$$

The restriction to the isotropic case implies that the free energy takes the separable form (see, for example Reese and Govindjee[45])

$$\Psi = \Psi(\mathbf{F}, \tau, \mathbf{C}_p^{-1}) = \Psi^{\mathrm{eq}}(\mathbf{F}, \tau) + \Psi^{\mathrm{neq}}(\mathbf{F}, \tau, \mathbf{C}_p^{-1}), \tag{28}$$

where Ψ^{eq} is the equilibrium part and Ψ^{neq} is the non-equilibrium part.

Since inelastic deformations are purely irreversible in nature, they lead to a contribution to the dissipative bracket in GENERIC (1), cf. (8). To derive the inelastic dissipative bracket (12), we resort to the dissipative bracket derived in Hütter and Svendsen[24] within a temperature-based framework for GENERIC. In particular, Hütter and Svendsen[24] consider functionals of the form

$$\overline{A}(\boldsymbol{\varphi}, \mathbf{p}, \theta, \mathbf{F}_p) = \int_{B} \overline{a}(\boldsymbol{\varphi}, \mathbf{F}, \mathbf{p}, \theta, \mathbf{F}_p) \, \mathrm{d}V, \tag{29}$$

with associated density function $\overline{a}(\boldsymbol{\varphi}, \mathbf{F}, \mathbf{p}, \theta, \mathbf{F}_p)$. The inelastic dissipative bracket from Hütter and Svendsen[24] is given by

$$\left[\overline{A}, \overline{B}\right]_{\mathrm{inel}} = \int_{B} \left(\frac{\delta_\theta \overline{a}}{\partial_\theta \overline{u}} \partial_{\mathbf{F}_p} \overline{u} - \delta_{\mathbf{F}_p} \overline{a}\right) : \Theta\mathbf{N} : \left(\frac{\delta_\theta \overline{b}}{\partial_\theta \overline{u}} \partial_{\mathbf{F}_p} \overline{u} - \delta_{\mathbf{F}_p} \overline{b}\right) \, \mathrm{d}V, \tag{30}$$

where $\overline{u}(\mathbf{F}, \theta, \mathbf{F}_p)$ is the internal energy density and $\mathbf{N}$ is a fourth-order inelastic flow tensor which has the properties $\mathbf{N}^{\mathrm{T}} = \mathbf{N}$ (major symmetry) and $\mathbf{A} : \mathbf{N} : \mathbf{A} \geq 0$ for all $\mathbf{A} \in \mathbb{R}^{3\times3}$. In components, these properties read

$$(\mathbf{N})^{\alpha\cdot\beta\cdot}_{\cdot I\cdot J} = (\mathbf{N})^{\beta\cdot\alpha\cdot}_{\cdot J\cdot I} \qquad \text{and} \qquad (\mathbf{A})^{\cdot I}_{\alpha\cdot} \, (\mathbf{N})^{\alpha\cdot\ \beta\cdot}_{\cdot I\cdot J} \, (\mathbf{A})^{\cdot J}_{\beta\cdot} \geq 0. \tag{31}$$

As has been shown in Hütter and Svendsen,[24] inelastic dissipative bracket (30) comes along with the flow rule

$$\dot{\mathbf{F}}_p = -\mathbf{N} : \boldsymbol{\Sigma},$$

where

$$\boldsymbol{\Sigma} = \partial_{\mathbf{F}_p} \overline{u} - \Theta \partial_{\mathbf{F}_p} \overline{\eta}.$$

In the last equation, $\overline{\eta}(\mathbf{F}, \theta, \mathbf{F}_p)$ is the entropy density of the temperature-based formulation.

3.1 | Change of variables

We perform a change of variables to transform the inelastic bracket (30) to the present setting which is based on functionals of the form (4). In particular, to link the current density functions $a(\boldsymbol{\varphi}, \mathbf{F}, \mathbf{p}, \tau, \mathbf{C}_p^{-1})$ to those in (29), we express the generalized thermodynamic variable $\tau \in \{\theta, \eta, u\}$ in terms of the temperature by inverting relation (10) to get

$$\tau = \overline{\tau}(\mathbf{F}, \theta, \mathbf{C}_p^{-1}). \tag{32}$$

Moreover, relation (27) implies

$$\mathbf{C}_p^{-1} = \mathbf{F}_p^{-1} \mathbf{F}_p^{-T}. \tag{33}$$

Now, the two density functions under consideration can be connected through

$$\overline{a}(\boldsymbol{\varphi}, \mathbf{F}, \mathbf{p}, \theta, \mathbf{F}_p) = a(\boldsymbol{\varphi}, \mathbf{F}, \mathbf{p}, \overline{\tau}(\mathbf{F}, \theta, \mathbf{C}_p^{-1}), \mathbf{C}_p^{-1}),$$

where relationships (32) and (33) are employed on the right-hand side of the last equation. A straightforward application of the chain rule to the last equation yields

$$\partial_\theta \overline{a} = \partial_\tau a \partial_\theta \overline{\tau}$$
$$\partial_{\mathbf{F}_p} \overline{a} = \partial_{\mathbf{F}_p} a + \partial_\tau a \partial_{\mathbf{F}_p} \overline{\tau}. \tag{34}$$

Note that $\delta_\theta \overline{a} = \partial_\theta \overline{a}$, and $\delta_{\mathbf{F}_p} \overline{a} = \partial_{\mathbf{F}_p} \overline{a}$. Furthermore, with regard to (10) and (32) we have $\theta = \Theta(\mathbf{F}, \overline{\tau}(\mathbf{F}, \theta, \mathbf{C}_p^{-1}), \mathbf{C}_p^{-1})$, from which follows that

$$1 = \partial_\theta \Theta = \partial_\tau \Theta \partial_\theta \overline{\tau},$$
$$\mathbf{0} = \partial_{\mathbf{F}_p} \Theta = \partial_\tau \Theta \partial_{\mathbf{F}_p} \overline{\tau} + \partial_{\mathbf{F}_p} \Theta.$$

We thus obtain

$$\partial_\theta \overline{\tau} = \frac{1}{\partial_\tau \Theta},$$
$$\partial_{\mathbf{F}_p} \overline{\tau} = -\frac{\partial_{\mathbf{F}_p} \Theta}{\partial_\tau \Theta}. \tag{35}$$

Substituting from (35) into (34) yields

$$\partial_\theta \overline{a} = \frac{\partial_\tau a}{\partial_\tau \Theta},$$
$$\partial_{\mathbf{F}_p} \overline{a} = \partial_{\mathbf{F}_p} a - \frac{\partial_\tau a}{\partial_\tau \Theta} \partial_{\mathbf{F}_p} \Theta. \tag{36}$$

Note that $\delta_\tau a = \partial_\tau a$ and $\delta_{\mathbf{F}_p} a = \partial_{\mathbf{F}_p} a$. Making use of (36), the terms in the parenthesis of (30) can be rewritten as

$$\frac{\delta_\theta \overline{a}}{\partial_\theta \overline{u}} \partial_{\mathbf{F}_p} \overline{u} - \delta_{\mathbf{F}_p} \overline{a} = \frac{\delta_\tau a}{\partial_\tau u} \partial_{\mathbf{F}_p} u - \delta_{\mathbf{F}_p} a. \tag{37}$$

Taking into account the relationship

$$\partial_{\mathbf{F}_p} a = -2 \mathbf{F}_p^{-T} \partial_{\mathbf{C}_p^{-1}} a \mathbf{C}_p^{-1}, \tag{38}$$

the inelastic dissipative bracket (30) can be recast in the form

$$[\mathcal{A}, \mathcal{B}]_{\text{inel}} = \int_B 2 \left(\frac{\delta_\tau a}{\partial_\tau u} \partial_{\mathbf{C}_p^{-1}} u \mathbf{C}_p^{-1} - \delta_{\mathbf{C}_p^{-1}} a \mathbf{C}_p^{-1} \right) : \Theta \mathcal{N} : 2 \left(\frac{\delta_\tau b}{\partial_\tau u} \partial_{\mathbf{C}_p^{-1}} u \mathbf{C}_p^{-1} - \delta_{\mathbf{C}_p^{-1}} b \mathbf{C}_p^{-1} \right) \, \mathrm{d}V.$$

This bracket coincides with the one introduced in (12). Note that in the above formula, $\delta_{\mathbf{C}_p^{-1}} a = \partial_{\mathbf{C}_p^{-1}} a$. Moreover, $\mathcal{N}$ is the material form of the fourth-order flow tensor N in (30). In components,

$$(\mathcal{N})_{\cdot J \cdot L}^{I \cdot K \cdot} = (\mathbf{F}_p^{-1})_{\cdot \alpha}^{I \cdot}(\mathbf{F}_p^{-1})_{\cdot \gamma}^{K \cdot}(\mathbf{N})_{\cdot J \cdot L}^{\alpha \cdot \gamma \cdot}. \tag{39}$$

Accordingly, the material flow tensor inherits symmetry and positive semi-definiteness. That is, in components,

$$(\mathcal{N})_{\cdot J \cdot L}^{I \cdot K \cdot} = (\mathcal{N})_{\cdot L \cdot J}^{K \cdot I \cdot} \qquad \text{and} \qquad (\mathbf{M})_{I \cdot}^{\cdot J} (\mathcal{N})_{\cdot J \cdot L}^{I \cdot K \cdot} (\mathbf{M})_{K \cdot}^{\cdot L} \geq 0 \tag{40}$$

for all $\mathbf{M}$ introduced in (17). As has been shown in Section 2.1, the above inelastic dissipative bracket gives rise to flow rules of the form (cf. (20)$_4$)

$$\overline{\dot{\mathbf{C}}_p^{-1}} = -2 \left(\mathcal{N} : \mathbf{M} \right) \mathbf{C}_p^{-1}. \tag{41}$$

It is worth noting that this flow rule can be viewed as material version of the viscoelastic evolution equation

$$\mathcal{L}_v \mathbf{b}_e = -2 \left(\mathcal{V}^{-1} : \tau^{\text{neq}} \right) \mathbf{b}_e, \tag{42}$$

derived in Reese and Govindjee[43,45] and applied in, for example, Budday et al.[46] In the last equation, $\mathbf{b}_e = \mathbf{F}_e \mathbf{F}_e^{\text{T}} = \mathbf{F} \mathbf{C}_p^{-1} \mathbf{F}^{\text{T}}$, $\mathcal{L}_v \mathbf{b}_e = \mathbf{F} \overline{\dot{\mathbf{C}}_p^{-1}} \mathbf{F}^{\text{T}}$, $\tau^{\text{neq}} = 2 \mathbf{F} \partial_{\mathbf{C}} \Psi^{\text{neq}} \mathbf{F}^{\text{T}}$, and $\mathcal{V}^{-1}$ is an isotropic, positive definite fourth-order tensor. Using these relationships, flow rule (42) can be recast in the form

$$\overline{\dot{\mathbf{C}}_p^{-1}} = -2 \mathbf{F}^{-1} \left(\mathcal{V}^{-1} : \left(\mathbf{F}^{-\text{T}} \mathbf{M} \mathbf{F}^{\text{T}} \right) \right) \mathbf{F} \mathbf{C}_p^{-1}, \tag{43}$$

where the relation

$$2 \mathbf{C} \partial_{\mathbf{C}} \Psi^{\text{neq}} = 2 \partial_{\mathbf{C}_p^{-1}} \Psi^{\text{neq}} \mathbf{C}_p^{-1} = \mathbf{M}$$

has been employed. Note that in the last equation, definition (17) of the Mandel stress tensor has been taken into account. Comparing (43) with present flow rule (41), leads to the conclusion that the respective fourth-order flow tensors are related by

$$(\mathcal{N})_{\cdot J \cdot L}^{I \cdot K \cdot} = (\mathbf{F}^{-1})_{\cdot a}^{I \cdot}(\mathbf{F})_{\cdot J}^{b \cdot}(\mathbf{F}^{-1})_{\cdot c}^{K \cdot}(\mathbf{F})_{\cdot L}^{d \cdot}(\mathcal{V}^{-1})_{\cdot b \cdot d}^{a \cdot c \cdot}.$$

We further remark that the present viscoelastic evolution equation (41) can also be brought into the form

$$\dot{\mathbf{C}}_p = 2 \mathbf{C}_p \mathcal{N} : \mathbf{M}.$$

This version of the viscoelastic evolution equation has been used in Krüger et al.;[29] see also Groß et al.[16] Thus we conclude that the newly proposed inelastic dissipative bracket (12) gives rise to evolution equations for the internal variables that have been previously developed in the context of finite deformation thermo-viscoelasticity.

4 | DISCRETIZATION IN SPACE

Concerning the space discretization of the present GENERIC-based formulation, we essentially apply an isoparametric finite element approach (see, for example, Hughes[47]). Our main goal is to achieve a GENERIC-consistent space discretization in the sense of Betsch and Schiebl.[40] In particular, a GENERIC-consistent space discretization ensures that the discrete formulation inherits the fundamental balance laws for both the energy and the entropy from the underlying continuous formulation (cf. Section 2.3).

We first restate the governing equations of the IBVP to be discretized in space and time. With regard to the GENERIC-based weak form (21), we consider the following set of equations:

$$0 = \dot{\boldsymbol{\varphi}} - \mathbf{v},$$

$$0 = \overline{\dot{\mathbf{C}}_p^{-1}} + 2 \left(\mathcal{N} : \mathbf{M} \right) \mathbf{C}_p^{-1},$$

$$0 = \int_{\mathcal{B}} w_{u_\tau} \left(\partial_\tau u - u_\tau \right) \, dV,$$

$$0 = \int_{\mathcal{B}} w_{\eta_\tau} \left(\partial_\tau \eta - \eta_\tau \right) \, dV,$$

$$\mathbf{0} = \int_{\mathcal{B}} \left(\mathbf{w_p} \cdot (\rho \dot{\mathbf{v}} - \mathbf{b}) + \mathbf{P} : \nabla \mathbf{w_p} \right) \, dV - \int_{\partial_\sigma \mathcal{B}} \mathbf{w_p} \cdot \bar{\mathbf{t}} \, dA,$$

$$0 = \int_{\mathcal{B}} w_\tau \left(\dot{\tau} - \frac{2}{u_\tau} \left(\partial_{\mathbf{C}_p^{-1}} u \mathbf{C}_p^{-1} \right) : \mathcal{N} : \mathbf{M} + \frac{1}{\eta_\tau} \partial_\mathbf{F} \eta : \nabla \mathbf{v} \right) \, dV$$

$$- \int_{\mathcal{B}} \nabla \left(\frac{w_\tau}{u_\tau} \right) \cdot \mathbf{Q} \, dV + \int_{\partial_q \mathcal{B}} \frac{w_\tau}{u_\tau} \bar{q} \, dA \, dV. \tag{44}$$

Here, the first equation represents the local form of the kinematic relationship $\dot{\boldsymbol{\varphi}} = \mathbf{v}$, while the second equation is the viscoelastic evolution equation. The third and fourth equation serve the purpose to introduce the new fields u_τ and η_τ. This procedure facilitates a mixed finite element approach which turns out to be crucial for a GENERIC-consistent discrete formulation. Due to the arbitrariness of the test functions w_{u_τ} and w_{η_τ}, $(44)_3$ and $(44)_4$ impose the conditions $u_\tau = \partial_\tau u$ and $\eta_\tau = \partial_\tau \eta$, respectively. Moreover,

$$\mathbf{P} = \partial_\mathbf{F} u - \Theta \partial_\mathbf{F} \eta,$$

$$\mathbf{M} = 2 \left(\partial_{\mathbf{C}_p^{-1}} u - \Theta \partial_{\mathbf{C}_p^{-1}} \eta \right) \mathbf{C}_p^{-1} \tag{45}$$

are the GENERIC-specific representations of the first Piola-Kirchhoff stress tensor and the material Mandel stress tensor previously introduced in (14) and (17), respectively. Similarly, the material heat flux vector $\mathbf{Q}$ has been introduced in (16). We emphasize again that the GENERIC-based formulation is based on expression (10) for the temperature field. In the present mixed formulation this implies

$$\Theta = \frac{u_\tau}{\eta_\tau}. \tag{46}$$

The finite element method is based on finite-dimensional approximations of the following quantities

$$\boldsymbol{\varphi}^h = N^a \mathbf{q}_a,$$
$$\mathbf{v}^h = N^a \mathbf{v}_a,$$
$$\tau^h = N^a \tau_a, \tag{47}$$

and

$$u_\tau^h = N^a (u_\tau)_a,$$
$$\eta_\tau^h = N^a (\eta_\tau)_a. \tag{48}$$

As before, the summation convention applies, where $a = 1, \ldots, \mathrm{N}$, and N denotes the total number of nodes in the finite element mesh. Moreover, $N^a : \mathcal{B} \to \mathbb{R}$ are the nodal shape functions with associated nodal values $\mathbf{q}_a, \mathbf{v}_a \in \mathbb{R}^3$ and $\tau_a, (u_\tau)_a, (\eta_\tau)_a \in \mathbb{R}$. Analogous approximations are used for the test functions $w_{u_\tau}, w_{\eta_\tau}, \mathbf{w_p}$, and w_τ, denoted by $w_{u_\tau}^h, w_{\eta_\tau}^h, \mathbf{w_p}^h$, and w_τ^h.

In what follows, we summarize the space-discrete version of (44). Nodal collocation of kinematic equation $(44)_1$ yields

$$\dot{\mathbf{q}}_a = \mathbf{v}_a, \tag{49}$$

for $a = 1, \ldots, \mathrm{N}$. Viscoelastic evolution equation $(44)_2$ is collocated at the integration points $\mathbf{X}_g \in \mathcal{B}$ used for the numerical evaluation of the volume integrals in (44). Accordingly,

$$\overline{(\mathbf{C}_p^{-1})}_g = -2 \left(\mathcal{N}_g : \mathbf{M}_g \right) (\mathbf{C}_p^{-1})_g, \tag{50}$$

for $g = 1, \ldots, G$, where G denotes the total number of integration points. Here and in the sequel, index g indicates evaluation at the integration point $\mathbf{X}_g \in \mathcal{B}$. For example,

$$(\mathbf{C}_p^{-1})_g = \mathbf{C}_p^{-1}(\mathbf{X}_g, t),$$
$$\mathbf{M}_g = 2 \left(\partial_{\mathbf{C}_p^{-1}} u_g - \Theta_g \partial_{\mathbf{C}_p^{-1}} \eta_g \right) (\mathbf{C}_p^{-1})_g, \tag{51}$$

where

$$u_g = u \left(\mathbf{F}_g^{\mathrm{h}}, \tau_g^{\mathrm{h}}, (\mathbf{C}_p^{-1})_g \right),$$
$$\eta_g = \eta \left(\mathbf{F}_g^{\mathrm{h}}, \tau_g^{\mathrm{h}}, (\mathbf{C}_p^{-1})_g \right), \tag{52}$$

are the internal energy and entropy densities at point $\mathbf{X}_g$. Furthermore, the discrete deformation gradient at $\mathbf{X}_g$, $\mathbf{F}_g^{\mathrm{h}}$, and the discrete generalized thermal variable, τ_g^{h}, follow from $(47)_{1,3}$ and thus take the form

$$\mathbf{F}_g^{\mathrm{h}} = \mathbf{q}_a(t) \otimes \nabla N^a(\mathbf{X}_g),$$
$$\tau_g^{\mathrm{h}} = N^a(\mathbf{X}_g)\tau_a(t). \tag{53}$$

Similarly, the discrete temperature at $\mathbf{X}_g$ follows from (46) and is given by

$$\Theta_g = \frac{(u_\tau^{\mathrm{h}})_g}{(\eta_\tau^{\mathrm{h}})_g} \tag{54}$$

where, in view of interpolations (48), $(u_\tau^{\mathrm{h}})_g = u_\tau^{\mathrm{h}}(\mathbf{X}_g, t)$ and $(\eta_\tau^{\mathrm{h}})_g = \eta_\tau^{\mathrm{h}}(\mathbf{X}_g, t)$. In the discrete setting, the fields u_τ^{h} and η_τ^{h} are determined through $(44)_{3,4}$. In particular, inserting the approximations (48) along with the corresponding formulas for $\mathrm{w}_{u_\tau}^{\mathrm{h}}$, $\mathrm{w}_{\eta_\tau}^{\mathrm{h}}$ into $(44)_{3,4}$, we obtain

$$0 = \sum_{g=1}^{G} N^a(\mathbf{X}_g) \left(\partial_\tau u_g - N^b(\mathbf{X}_g)(u_\tau)_b \right) w_g,$$
$$0 = \sum_{g=1}^{G} N^a(\mathbf{X}_g) \left(\partial_\tau \eta_g - N^b(\mathbf{X}_g)(u_\tau)_b \right) w_g, \tag{55}$$

for $a = 1, \ldots, N$. To calculate the spatial integrals, appropriate numerical quadrature formulas of the form

$$\int_{\mathcal{B}} f(\mathbf{X}) \, \mathrm{d}V \approx \sum_{g=1}^{G} f(\mathbf{X}_g) w_g \tag{56}$$

have been applied to obtain (55).[*] Here, w_g play the role of generalized weighting coefficients resulting from the specific quadrature rule along with the isoparametric description of reference domain $\mathcal{B}$. Now, $(55)_1$ can be solved for the nodal quantities $(u_\tau)_a$, $a = 1, \ldots, N$. To this end, we introduce the components H^{ab} of the positive definite Gram matrix $[H^{ab}]$,

$$H^{ab} = \sum_{g=1}^{G} N^a(\mathbf{X}_g) N^b(\mathbf{X}_g) w_g, \tag{57}$$

so that $(55)_1$ can be rewritten as

$$H^{ab}(u_\tau)_b = \sum_{g=1}^{G} N^a(\mathbf{X}_g) \partial_\tau u_g w_g. \tag{58}$$

The components H_{ab} of the inverse Gram matrix, $[H_{ab}] = [H^{ab}]^{-1}$, satisfy the relationship

$$H_{ab} H^{bc} = \delta_a^c, \tag{59}$$

---

[*]The summation over g will always be stated explicitly, so that the summation convention does not apply to index g.

where δ^c_a denotes the Kronecker delta. Now, interpolation formula $(48)_1$ along with (58) lead to the result

$$u^{\rm h}_\tau = N^a H_{ab} \sum_{g=1}^{G} N^b(\mathbf{X}_g) \partial_\tau u_g w_g,$$

(60)

which will be utilized below. Similarly, interpolation formula $(48)_2$ in conjunction with $(55)_2$ yield the result

$$\eta^{\rm h}_\tau = N^a H_{ab} \sum_{g=1}^{G} N^b(\mathbf{X}_g) \partial_\tau \eta_g w_g.$$

(61)

Next, we turn to the discretization of $(44)_5$, which can be done in a straightforward way to obtain

$$M^{ab} \dot{\mathbf{v}}_b - \sum_{g=1}^{G} N^a(\mathbf{X}_g) \mathbf{b}_g w_g + \sum_{g=1}^{G} \mathbf{P}_g \nabla N^a(\mathbf{X}_g) w_g = 0.$$

(62)

For simplicity, we have neglected the contribution of the external tractions which could be easily added to the above equation. In the above equation, first Piola-Kirchhoff stress tensor $\mathbf{P}_g$ at point $\mathbf{X}_g \in \mathcal{B}$ is given by

$$\mathbf{P}_g = \partial_{\mathbf{F}} u_g - \Theta_g \partial_{\mathbf{F}} \eta_g.$$

(63)

Moreover, in (62), the components M^{ab} of the mass matrix are given by

$$M^{ab} = \sum_{g=1}^{G} \rho(\mathbf{X}_g) N^a(\mathbf{X}_g) N^b(\mathbf{X}_g) w_g.$$

(64)

We further introduce nodal momentum vectors $\mathbf{p}^a$ conjugate to nodal position vectors $\mathbf{q}_a$ through the standard relation

$$\mathbf{p}^a = M^{ab} \mathbf{v}_a.$$

(65)

Eventually, we consider the space-discrete version of $(44)_6$. Straight-forward application of our approach yields

$$0 = H^{ab} \dot{\tau}_b - \sum_{g=1}^{G} \frac{2N^a(\mathbf{X}_g)}{(u^{\rm h}_\tau)_g} \left(\partial_{\mathbf{C}_p^{-1}} u_g (\mathbf{C}_p^{-1})_g \right) : \mathcal{N}_g : \mathbf{M}_g w_g$$

$$+ \mathbf{v}_c \cdot \sum_{g=1}^{G} \frac{N^a(\mathbf{X}_g)}{(\eta^{\rm h}_\tau)_g} \partial_{\mathbf{F}} \eta_g \nabla N^c(\mathbf{X}_g) w_g - \sum_{g=1}^{G} \nabla \left(\frac{N^a(\mathbf{X}_g)}{(u^{\rm h}_\tau)_g} \right) \cdot \mathbf{Q}_g w_g,$$

(66)

where the material heat flux vector $\mathbf{Q}_g$ at point $\mathbf{X}_g \in \mathcal{B}$ is given by

$$\mathbf{Q}_g = \Theta^2_g \mathbf{K}_g \nabla \left(\frac{(\eta^{\rm h}_\tau)_g}{(u^{\rm h}_\tau)_g} \right).$$

For simplicity, in the space-discrete evolution equation (66) for the generalized nodal thermal variable τ_b, the term accounting for heat transfer across the boundary has been neglected. To summarize, the resulting evolution equations for the space-discrete system at hand can be written in the form

$$\dot{\mathbf{q}}_a = M_{ab} \mathbf{p}^b,$$

$$\dot{\mathbf{p}}^a = \sum_{g=1}^{G} N^a(\mathbf{X}_g) \mathbf{b}_g w_g - \sum_{g=1}^{G} \mathbf{P}_g \nabla N^a(\mathbf{X}_g) w_g,$$

$$\dot{\tau}_a = H_{ab} \sum_{g=1}^{G} \frac{2N^b(\mathbf{X}_g)}{(u^{\rm h}_\tau)_g} \left(\partial_{\mathbf{C}_p^{-1}} u_g (\mathbf{C}_p^{-1})_g \right) : \mathcal{N}_g : \mathbf{M}_g w_g$$

$$-\mathbf{v}_c \cdot H_{ab} \sum_{g=1}^{G} \frac{N^b(\mathbf{X}_g)}{(\eta_\tau^h)_g} \partial_\mathbf{F}\eta_g \nabla N^c(\mathbf{X}_g) w_g + H_{ab} \sum_{g=1}^{G} \nabla\left(\frac{N^b(\mathbf{X}_g)}{(u_\tau^h)_g}\right) \mathbf{Q}_g w_g,$$

$$(\dot{\overline{\mathbf{C}_p^{-1}}})_g = -2\left(\mathcal{N}_g : \mathbf{M}_g\right)(\mathbf{C}_p^{-1})_g, \tag{67}$$

for $1, \dots, N$ and $1, \dots, G$. In $(67)_1$, M_{ab} stands for the components of the inverse mass matrix satisfying $M_{ab}M^{bc} = \delta_a^c$. The set of Equation (67) constitutes nonlinear first-order ordinary differential equations for the determination of the unknowns which can be collected in the state vector

$$\mathbf{z} = \left(\mathbf{q}_1, \dots \mathbf{q}_N, \mathbf{p}^1, \dots \mathbf{p}^N, \tau_1, \dots \tau_N, (\mathbf{C}_p^{-1})_1^{AB}, \dots (\mathbf{C}_p^{-1})_G^{AB}\right). \tag{68}$$

In the sequel, state vector (68) will be viewed as column vector. In particular, this implies that the six independent components $(\mathbf{C}_p^{-1})_g^{AB}, g = 1, \dots, G$, of the internal variable $(\mathbf{C}_p^{-1})_g$ (at quadrature point $\mathbf{X}_g$) are arranged in a column vector. The set of evolution equations (67) fits into the GENERIC framework for discrete systems, as shown next.

4.1 | GENERIC-consistent space discretization

Our discretization approach presented above is GENERIC-consistent in the sense of Betsch and Schiebl[40] and thus can be framed in the context of GENERIC for discrete systems. To see this, the set of evolution equation (67) needs to be put into the form

$$\dot{\mathbf{z}} = \mathbf{L}\nabla\mathcal{E}(\mathbf{z}) + \mathbf{M}\nabla\mathcal{S}(\mathbf{z}). \tag{69}$$

Here, the focus is again on closed systems in which the boundary contributions are disregarded. In analogy to (1), the time-evolution of the state vector is decomposed additively into a reversible part generated by the total energy $\mathcal{E}$ and an irreversible part generated by the total entropy $\mathcal{S}$. Poisson matrix $\mathbf{L}$ needs be skew-symmetric, while friction matrix $\mathbf{M}$ needs be symmetric positive semi-definite.

In the above equation, the total energy of the discrete system under consideration is given by

$$\mathcal{E}(\mathbf{z}) = \frac{1}{2}M_{ab}\mathbf{p}^a \cdot \mathbf{p}^b + \sum_{g=1}^{G}\left[u\left(\mathbf{F}_g^h, \tau_g^h, (\mathbf{C}_p^{-1})_g\right) - \mathbf{q}_a N^a(\mathbf{X}_g)\mathbf{b}(\mathbf{X}_g)\right] w_g. \tag{70}$$

This is the space-discrete version of total energy (11). Similarly, the space-discrete version of total entropy (7) takes the form

$$\mathcal{S}(\mathbf{z}) = \sum_{g=1}^{G}\eta\left(\mathbf{F}_g^h, \tau_g^h, (\mathbf{C}_p^{-1})_g\right) w_g. \tag{71}$$

To get the gradient of the total energy, $\nabla\mathcal{E}(\mathbf{z})$, we consider the derivative of (70) with respect to time. Accordingly, the left-hand side of (70) yields

$$\frac{d}{dt}\mathcal{E}(\mathbf{z}) = \partial_{\mathbf{q}_a}\mathcal{E} \cdot \dot{\mathbf{q}}_a + \partial_{\mathbf{p}^a}\mathcal{E} \cdot \dot{\mathbf{p}}^a + \partial_{\tau_a}\mathcal{E} \cdot \dot{\tau}_a + \sum_{g=1}^{G}\partial_{(\mathbf{C}_p^{-1})_g^{AB}}\mathcal{E} \,(\dot{\overline{\mathbf{C}_p^{-1}}})_g^{AB}, \tag{72}$$

while the right-hand side of (70) gives

$$\frac{d}{dt}\mathcal{E}(\mathbf{z}) = \dot{\mathbf{p}}^a \cdot \mathbf{p}^b M_{ab} + \dot{\mathbf{q}}_a \cdot \sum_{g=1}^{G}\left[\partial_\mathbf{F}u_g \nabla N^a(\mathbf{X}_g) - N^a(\mathbf{X}_g)\mathbf{b}(\mathbf{X}_g)\right] w_g$$

$$+ \dot{\tau}_a \sum_{g=1}^{G}N^a(\mathbf{X}_g)\partial_\tau u_g w_g + \sum_{g=1}^{G}w_g \partial_{\mathbf{C}_p^{-1}}u_g : (\dot{\overline{\mathbf{C}_p^{-1}}})_g. \tag{73}$$

Comparing (72) with (73) yields the following expressions for the respective derivatives of the total energy

$$\partial_{\mathbf{q}_a}\mathcal{E} = \sum_{g=1}^{G} \left[\partial_{\mathbf{F}}u_g\nabla N^a(\mathbf{X}_g) - N^a(\mathbf{X}_g)\mathbf{b}(\mathbf{X}_g)\right]w_g,$$

$$\partial_{\mathbf{p}^a}\mathcal{E} = M_{ab}\mathbf{p}^b,$$

$$\partial_{\tau_a}\mathcal{E} = \sum_{g=1}^{G}N^a(\mathbf{X}_g)\partial_\tau u_g w_g,$$

$$\frac{\partial\mathcal{E}}{\partial(\mathbf{C}_p^{-1})_g^{AB}} = w_g\frac{\partial u_g}{\partial(\mathbf{C}_p^{-1})^{AB}}. \tag{74}$$

In particular, inserting from $(74)_3$ into (60), we obtain the important relationship

$$u_\tau^{\mathrm{h}} = N^a H_{ab}\partial_{\tau_b}\mathcal{E}. \tag{75}$$

Similarly, the derivatives of total entropy (71) take the form

$$\partial_{\mathbf{q}_a}\mathcal{S} = \sum_{g=1}^{G}\partial_{\mathbf{F}}\eta_g\nabla N^a(\mathbf{X}_g)w_g,$$

$$\partial_{\mathbf{p}^a}\mathcal{S} = \mathbf{0},$$

$$\partial_{\tau_a}\mathcal{S} = \sum_{g=1}^{G}N^a(\mathbf{X}_g)\partial_\tau\eta_g w_g,$$

$$\frac{\partial\mathcal{S}}{\partial(\mathbf{C}_p^{-1})_g^{AB}} = w_g\frac{\partial\eta_g}{\partial(\mathbf{C}_p^{-1})^{AB}}. \tag{76}$$

Inserting from $(76)_3$ into (61), we obtain

$$\eta_\tau^{\mathrm{h}} = N^a H_{ab}\partial_{\tau_b}\mathcal{S}. \tag{77}$$

Now, guided by discrete GENERIC (69), the evolution equations in (67) can be recast. In particular, taking into account $(74)_2$, kinematic relation $(67)_1$ can be rewritten as

$$\dot{\mathbf{q}}_a = \partial_{\mathbf{p}^a}\mathcal{E}. \tag{78}$$

Next, evolution equation $(67)_2$ for the nodal momentum vectors together with (63) and (54) yields

$$\dot{\mathbf{p}}^a = -\sum_{g=1}^{G}\left[\partial_{\mathbf{F}}u_g\nabla N^a(\mathbf{X}_g) - N^a(\mathbf{X}_g)\mathbf{b}(\mathbf{X}_g)\right]w_g + \sum_{g=1}^{G}\frac{(u_\tau^{\mathrm{h}})_g}{(\eta_\tau^{\mathrm{h}})_g}\partial_{\mathbf{F}}\eta_g\nabla N^a(\mathbf{X}_g)w_g.$$

Taking into account $(74)_1$ and (75), we obtain

$$\dot{\mathbf{p}}^a = -\partial_{\mathbf{q}_a}\mathcal{E} + \partial_{\tau_b}\mathcal{E}\,H_{bc}\sum_{g=1}^{G}\frac{N^c(\mathbf{X}_g)}{(\eta_\tau^{\mathrm{h}})_g}\partial_{\mathbf{F}}\eta_g\nabla N^a(\mathbf{X}_g)w_g. \tag{79}$$

Concerning the evolution of the nodal thermal variable τ_a, $(67)_3$ along with $(51)_2$, (54), and (77) lead to

$$\dot{\tau}_a = H_{ab}\sum_{g=1}^{G}\frac{4N^b(\mathbf{X}_g)N^c(\mathbf{X}_g)}{(u_\tau^{\mathrm{h}})_g(\eta_\tau^{\mathrm{h}})_g}\left(\partial_{\mathbf{C}_p^{-1}}u_g(\mathbf{C}_p^{-1})_g\right) : \mathcal{N}_g : \left(\partial_{\mathbf{C}_p^{-1}}u_g(\mathbf{C}_p^{-1})_g\right)w_g\,H_{cd}\partial_{\tau_d}\mathcal{S}$$

$$- H_{ab}\sum_{g=1}^{G}\frac{4N^b(\mathbf{X}_g)}{(\eta_\tau^{\mathrm{h}})_g}\left(\partial_{\mathbf{C}_p^{-1}}\eta_g(\mathbf{C}_p^{-1})_g\right) : \mathcal{N}_g : \left(\partial_{\mathbf{C}_p^{-1}}u_g(\mathbf{C}_p^{-1})_g\right)w_g$$

$$- \partial_{\mathbf{p}^c} \mathcal{E} \cdot H_{ab} \sum_{g=1}^{G} \frac{N^b(\mathbf{X}_g)}{(\eta_\tau^{\mathrm{h}})_g} \partial_{\mathbf{F}} \eta_g \nabla N^c(\mathbf{X}_g) w_g$$

$$+ H_{ab} \sum_{g=1}^{G} \Theta_g^2 \nabla \left(\frac{N^b(\mathbf{X}_g)}{(u_\tau^{\mathrm{h}})_g} \right) \cdot \mathbf{K}_g \nabla \left(\frac{N^c(\mathbf{X}_g)}{(u_\tau^{\mathrm{h}})_g} \right) w_g \; H_{cd} \partial_{\tau_d} S. \tag{80}$$

Eventually, evolution equation $(67)_4$ for the internal variable, together with $(51)_2$, (54), and (77) result in

$$\overline{(\dot{\mathbf{C}}_p^{-1})}_g = -\frac{4N^a(\mathbf{X}_g)}{(\eta_\tau^{\mathrm{h}})_g} \left(\mathcal{N}_g : \left(\partial_{\mathbf{C}_p^{-1}} u_g(\mathbf{C}_p^{-1})_g \right) \right) (\mathbf{C}_p^{-1})_g \; H_{ab} \partial_{\tau_b} S$$

$$+ 4\Theta_g \left(\mathcal{N}_g : \left(\partial_{\mathbf{C}_p^{-1}} \eta_g(\mathbf{C}_p^{-1})_g \right) \right) (\mathbf{C}_p^{-1})_g. \tag{81}$$

Next, we aim at introducing relation $(76)_4$ into the last term of (81). To this end, we introduce the fourth-order tensor $\mathcal{M}$ with components

$$(\mathcal{M})^{ABIJ} = (\mathbf{C}_p^{-1})^{CB} (\mathcal{N})_{\cdot C \cdot K}^{A \cdot I \cdot} (\mathbf{C}_p^{-1})^{JK}. \tag{82}$$

Note that $\mathcal{M}$ enjoys major symmetry, $(\mathcal{M})^{ABIJ} = (\mathcal{M})^{IJAB}$, due to the major symmetry of the material flow tensor $\mathcal{N}$ and the symmetry of $\mathbf{C}_p^{-1}$. Now, (81) can be recast in index form

$$(\overline{\dot{\mathbf{C}}_p^{-1}})_g^{AB} = -4(\mathcal{M})_g^{ABIJ} \frac{\partial u_g}{\partial(\mathbf{C}_p^{-1})^{IJ}} \frac{N^a(\mathbf{X}_g)}{(\eta_\tau^{\mathrm{h}})_g} H_{ab} \; \partial_{\tau_b} S + 4\frac{\Theta_g}{w_g}(\mathcal{M})_g^{ABIJ} \frac{\partial S}{\partial(\mathbf{C}_p^{-1})_g^{IJ}}. \tag{83}$$

Altogether, evolution equation (67) pertaining to the state variables of the discrete system at hand can be recast in the form

$$\dot{\mathbf{q}}_a = \partial_{\mathbf{p}^a} \mathcal{E},$$

$$\dot{\mathbf{p}}^a = -\partial_{\mathbf{q}_a} \mathcal{E} + \mathbf{l}_{\cdot b}^{a \cdot} \; \partial_{\tau_b} \mathcal{E},$$

$$\dot{\tau}_a = -(\mathbf{l}_{\cdot a}^{b \cdot})^{\mathrm{T}} \; \partial_{\mathbf{p}^b} \mathcal{E} + m_{ab} \; \partial_{\tau_b} S + \sum_{g=1}^{G} m_{g,a}^{IJ} \frac{\partial S}{\partial(\mathbf{C}_p^{-1})_g^{IJ}},$$

$$(\overline{\dot{\mathbf{C}}_p^{-1}})_g^{AB} = m_{g,b}^{AB} \; \partial_{\tau_b} S + m_g^{ABIJ} \frac{\partial S}{\partial(\mathbf{C}_p^{-1})_g^{IJ}}, \tag{84}$$

where

$$\mathbf{l}_{\cdot b}^{a \cdot} = H_{bc} \sum_{g=1}^{G} \frac{N_g^c}{(\eta_\tau^{\mathrm{h}})_g} \partial_{\mathbf{F}} \eta_g \nabla N_g^a w_g,$$

$$m_{ab} = H_{ac} \sum_{g=1}^{G} \Theta_g^2 \nabla \left(\frac{N_g^c}{(u_\tau^{\mathrm{h}})_g} \right) \cdot \mathbf{K}_g \nabla \left(\frac{N_g^d}{(u_\tau^{\mathrm{h}})_g} \right) w_g \; H_{db}$$

$$+ H_{ac} \sum_{g=1}^{G} \frac{4N_g^c N_g^d}{(u_\tau^{\mathrm{h}})_g(\eta_\tau^{\mathrm{h}})_g} \frac{\partial u_g}{\partial(\mathbf{C}_p^{-1})^{AB}} (\mathcal{M})_g^{ABIJ} \frac{\partial u_g}{\partial(\mathbf{C}_p^{-1})^{IJ}} w_g \; H_{db},$$

$$m_{g,b}^{AB} = -4(\mathcal{M})_g^{ABIJ} \frac{\partial u_g}{\partial(\mathbf{C}_p^{-1})^{IJ}} \frac{N_g^a}{(\eta_\tau^{\mathrm{h}})_g} H_{ab},$$

$$m_g^{ABIJ} = 4\frac{\Theta_g}{w_g}(\mathcal{M})_g^{ABIJ}. \tag{85}$$

For simplicity of exposition, in (85), $N_g^a = N^a(\mathbf{X}_g)$. Note that the properties $m_{ab} = m_{ba}$ and $m_g^{ABIJ} = m_g^{IJAB}$ hold.

Now, evolution equations (84) give rise to specific forms of Poisson matrix $\mathbf{L}$ and friction matrix $\mathbf{M}$ in GENERIC (69). In particular, the Poisson matrix takes the form

$$
\mathbf{L} = \begin{bmatrix}
0 & I & 0 & 0 \\
-I & 0 & \left[\mathbf{l}^{a\cdot}_{\cdot b}\right] & 0 \\
0 & \left[-\mathbf{l}^{b\cdot}_{\cdot a}\right]^{\mathrm{T}} & 0 & 0 \\
0 & 0 & 0 & 0
\end{bmatrix}, \tag{86}
$$

where I is the identity matrix (with appropriate dimension corresponding to the partitioning of the state vector (68)), and matrix $[\mathbf{l}^{a\cdot}_{\cdot b}]$ consists of vectors $\mathbf{l}^{a\cdot}_{\cdot b}$ defined in (85)$_1$. Specifically, we have

$$
\left[\mathbf{l}^{a\cdot}_{\cdot b}\right] = \begin{bmatrix}
\mathbf{l}^{1\cdot}_{\cdot 1} & \cdots & \mathbf{l}^{1\cdot}_{\cdot N} \\
\vdots & \ddots & \vdots \\
\mathbf{l}^{N\cdot}_{\cdot 1} & \cdots & \mathbf{l}^{N\cdot}_{\cdot N}
\end{bmatrix}. \tag{87}
$$

It can be observed that Poisson matrix (86) is skew-symmetric. Furthermore, the friction matrix is given by

$$
\mathbf{M} = \begin{bmatrix}
0 & 0 & 0 & 0 \\
0 & 0 & 0 & 0 \\
0 & 0 & \left[m_{ab}\right] & \left[\mathbf{m}^{IJ}_{g,a}\right] \\
0 & 0 & \left[\mathbf{m}^{AB}_{g,b}\right]^{\mathrm{T}} & \left[\mathbf{m}^{ABIJ}_{g}\right]
\end{bmatrix}, \tag{88}
$$

Here, the block matrices $[m_{ab}] \in \mathbb{R}^{N \times N}$, $[\mathbf{m}^{IJ}_{g,b}] \in \mathbb{R}^{N \times 6G}$, and $[\mathbf{m}^{ABIJ}_{g}]$ contain the components defined in (85)$_{2-4}$ and take the form

$$
\left[m_{ab} \right] = \begin{bmatrix}
m_{11} & \cdots & m_{1N} \\
\vdots & \ddots & \vdots \\
m_{N1} & \cdots & m_{NN}
\end{bmatrix}, \qquad
\left[\mathbf{m}^{IJ}_{g,a} \right] = \begin{bmatrix}
[m^{IJ}_{1,1}] & \cdots & [m^{IJ}_{G,1}] \\
\vdots & \ddots & \vdots \\
[m^{IJ}_{1,N}] & \cdots & [m^{IJ}_{G,N}]
\end{bmatrix}
$$

and

$$
\left[\mathbf{m}^{ABIJ}_{g} \right] = \begin{bmatrix}
[m^{ABIJ}_{1}] & \cdots & 0 \\
\vdots & \ddots & \vdots \\
0 & \cdots & [m^{ABIJ}_{G}]
\end{bmatrix}.
$$

Note that the last matrix is block-diagonal and symmetric. It can be easily observed that friction matrix (88) is symmetric and positive semi-definite.

4.2 | Conservation properties

We next verify the conservation properties of the semi-discrete formulation of the closed system dealt with in Section 4.1. Since the evolution equations pertaining to the semi-discrete formulation can be brought into GENERIC form (69), (i) conservation of total energy, and (ii) non-decreasing total entropy are automatically satisfied. To see this, we first consider the time-derivative of the total energy,

$$
\begin{aligned}
\frac{\mathrm{d}}{\mathrm{d}t}\mathcal{E}(\mathbf{z}) &= \nabla\mathcal{E}(\mathbf{z})\dot{\mathbf{z}} \\
&= \nabla\mathcal{E}(\mathbf{z})\mathbf{L}\nabla\mathcal{E}(\mathbf{z}) + \nabla\mathcal{E}(\mathbf{z})\mathbf{M}\nabla\mathcal{S}(\mathbf{z}),
\end{aligned}
\tag{89}
$$

where (69) has been used. The first term on the right-hand side of the last equation vanishes due to the skew-symmetry of Poisson matrix (86). The second term vanishes too, since the non-interaction condition

$$
\mathbf{M}\nabla\mathcal{E}(\mathbf{z}) = \mathbf{0}
\tag{90}
$$

holds. The last equation can be easily verified by a straight-forward calculation. Accordingly, (89) yields the conservation law $\mathrm{d}\mathcal{E}/\mathrm{d}t = 0$. Similarly, the time-derivative of the total entropy yields

$$
\begin{aligned}
\frac{\mathrm{d}}{\mathrm{d}t}\mathcal{S}(\mathbf{z}) &= \nabla\mathcal{S}(\mathbf{z})\dot{\mathbf{z}} \\
&= \nabla\mathcal{S}(\mathbf{z})\mathbf{L}\nabla\mathcal{E}(\mathbf{z}) + \nabla\mathcal{S}(\mathbf{z})\mathbf{M}\nabla\mathcal{S}(\mathbf{z}).
\end{aligned}
\tag{91}
$$

It can be verified by a straight-forward calculation that the second non-interaction condition

$$
\mathbf{L}\nabla\mathcal{S}(\mathbf{z}) = \mathbf{0}
\tag{92}
$$

is satisfied. In addition to that, the positive semi-definiteness of friction matrix (88) implies the result $\mathrm{d}\mathcal{S}/\mathrm{d}t \geq 0$. In particular, this result represents the semi-discrete version of (25) (apart from the boundary term in (25) originating from heat flux across the boundary). Thus, the total entropy of the closed system at hand is non-decreasing, due to the irreversible nature of heat conduction and visco-elastic deformations.

Since the material response is assumed to be frame-indifferent (or objective), specific symmetry properties are inherent to the discrete system under consideration. In particular, invariance under rigid rotations implies satisfaction of the following conditions (see Appendix A for further details):

$$
\begin{aligned}
\mathbf{0} &= \mathbf{q}_a \times \partial_{\mathbf{q}_a}\mathcal{E}, \\
\mathbf{0} &= \mathbf{q}_a \times \mathbf{l}_b^a,
\end{aligned}
\tag{93}
$$

for all $b = 1, \ldots, N$. We tacitly assume that no resultant external torque is acting on the system (i.e., the right-hand side of (23) is assumed to vanish). The semi-discrete version of the angular momentum relative to the origin is given by

$$
\mathbf{J}^{\mathrm{h}} = \int_{\mathcal{B}} \rho\boldsymbol{\varphi}^{\mathrm{h}} \times \mathbf{v}^{\mathrm{h}}\,\mathrm{d}V = \mathbf{q}_a \times \mathbf{p}^a,
\tag{94}
$$

where formulas $(47)_{1,2}$ along with definition (65) of the nodal momentum vectors $\mathbf{p}^a$ have been used. The time-derivative of (94) reads

$$
\begin{aligned}
\frac{\mathrm{d}}{\mathrm{d}t}\mathbf{J}^{\mathrm{h}} &= \dot{\mathbf{q}}_a \times \mathbf{p}^a + \mathbf{q}_a \times \dot{\mathbf{p}}^a \\
&= M_{ab}\mathbf{p}^b \times \mathbf{p}^a + \mathbf{q}_a \times \left(-\partial_{\mathbf{q}_a}\mathcal{E} + \mathbf{l}_b^a\,\partial_{\tau_b}\mathcal{E}\right)
\end{aligned}
\tag{95}
$$

where $(67)_1$ and $(84)_2$ have been used. Now the right-hand side of the last equation vanishes due to (i) the symmetry of M_{ab} together with the skew-symmetry of the vector cross product, and (ii) symmetry conditions (93). Result $\mathrm{d}\mathbf{J}^{\mathrm{h}}/\mathrm{d}t = \mathbf{0}$ implies conservation of total angular momentum.

4.3 | Choice of the thermodynamic variable

We shortly outline the impact of the specific choice of the thermodynamic variable, $\tau \in \{\theta, \eta, u\}$, on the structure of GENERIC (69). For simplicity, in this section we neglect body forces, that is, $\mathbf{b} = \mathbf{0}$ and still focus on closed systems.

Choosing the internal energy density as thermodynamic variable, that is, $\tau = u$, the total energy (70) takes a particularly simple form given by

$$\hat{\mathcal{E}}(\mathbf{z}) = \frac{1}{2} M_{ab} \mathbf{p}^a \cdot \mathbf{p}^b + \sum_{g=1}^{G} u_g^{\mathrm{h}} w_g \tag{96}$$

As before, u_g^{h} stands for $u^{\mathrm{h}}(\mathbf{X}_g, t)$. In particular, interpolation formula $(53)_2$ gives rise to $u_g^{\mathrm{h}} = N^a(\mathbf{X}_g) u_a(t)$. The derivatives of the total energy in (74) simplify to

$$\partial_{\mathbf{q}_a} \hat{\mathcal{E}} = \mathbf{0},$$
$$\partial_{\mathbf{p}^a} \hat{\mathcal{E}} = M_{ab} \mathbf{p}^b,$$
$$\partial_{u_a} \hat{\mathcal{E}} = \sum_{g=1}^{G} N^a(\mathbf{X}_g) w_g,$$
$$\frac{\partial \hat{\mathcal{E}}}{\partial (\mathbf{C}_p^{-1})_g^{AB}} = 0. \tag{97}$$

Consequently,

$$\frac{\mathrm{d}}{\mathrm{d}t} \hat{\mathcal{E}}(\mathbf{z}) = \nabla \hat{\mathcal{E}}(\mathbf{z}) \dot{\mathbf{z}}$$
$$= M_{ab} \mathbf{p}^a \cdot \dot{\mathbf{p}}^b + \sum_{g=1}^{G} N^a(\mathbf{X}_g) \dot{u}_a w_g. \tag{98}$$

Moreover, for the choice $\tau = u$ friction matrix (88) attains a particularly simple block-diagonal form, since $m_{g,b}^{AB} = 0$, and coefficients m_{ab} only contain contributions due to heat conduction (cf. (85)).

Choosing the internal entropy density as thermodynamic variable, that is, $\tau = \eta$, yields a particularly simple form of the total entropy (71) given by

$$\tilde{S}(\mathbf{z}) = \sum_{g=1}^{G} \eta_g^{\mathrm{h}} w_g, \tag{99}$$

where interpolation formula $(53)_2$ gives rise to $\eta_g^{\mathrm{h}} = N^a(\mathbf{X}_g) \eta_a(t)$. Consequently, the derivatives of the total entropy in (76) simplify to

$$\partial_{\mathbf{q}_a} \tilde{S} = \mathbf{0},$$
$$\partial_{\mathbf{p}^a} \tilde{S} = \mathbf{0},$$
$$\partial_{\eta_a} \tilde{S} = \sum_{g=1}^{G} N^a(\mathbf{X}_g) w_g,$$
$$\frac{\partial \tilde{S}}{\partial (\mathbf{C}_p^{-1})_g^{AB}} = 0. \tag{100}$$

Thus

$$\frac{\mathrm{d}}{\mathrm{d}t} \tilde{S}(\mathbf{z}) = \nabla \tilde{S}(\mathbf{z}) \dot{\mathbf{z}}$$
$$= \sum_{g=1}^{G} N^a(\mathbf{X}_g) \dot{\eta}_a w_g. \tag{101}$$

Moreover, the choice $\tau = \eta$ leads to $\mathbf{l}_b^a = \mathbf{0}$ (see (85)), so that Poisson matrix (86) yields a particularly simple form.

In contrast to the above considerations, selecting the total temperature as thermodynamic variable, that is, $\tau = \theta$, essentially does not lead to any simplifications. We eventually remark that these conclusions also affect the discretization in time, which will be treated next.

5 | DISCRETIZATION IN TIME

We now turn to the discretization in time of the semi-discrete GENERIC-consistent evolution equations derived in Section 4.1. To this end, we focus on a representative time interval $[t_n, t_{n+1}]$ with corresponding time-step size $\Delta t = t_{n+1} - t_n$. We aim at second-order accurate, implicit time-stepping schemes based on the mid-point rule. Application of the mid-point rule to (69) yields

$$\mathbf{z}_{n+1} - \mathbf{z}_n = \Delta t \mathbf{L}(\mathbf{z}_{n+\frac{1}{2}}) \nabla \mathcal{E}(\mathbf{z}_{n+\frac{1}{2}}) + \Delta t \mathbf{M}(\mathbf{z}_{n+\frac{1}{2}}) \nabla \mathcal{S}(\mathbf{z}_{n+\frac{1}{2}}). \tag{102}$$

Here, $\mathbf{z}_n$ stands for the discrete vector of state variables at time t_n, and

$$\mathbf{z}_{n+\frac{1}{2}} = \frac{1}{2} (\mathbf{z}_n + \mathbf{z}_{n+1}).$$

Provided that the state variables $\mathbf{z}_n$ are given, the state variables $\mathbf{z}_{n+1}$ can be determined by solving (102).

5.1 | Partially structure-preserving schemes

Next, we check whether, or under what conditions, structure-preserving properties hold in the discrete setting. In this connection, we shall see that the specific choice of the thermodynamic variable $\tau \in \{\theta, \eta, u\}$ plays a crucial role. It can be easily verified that non-interaction conditions (90) and (92) are still satisfied in the sense that

$$\mathbf{M}(\mathbf{z}_{n+\frac{1}{2}}) \nabla \mathcal{E}(\mathbf{z}_{n+\frac{1}{2}}) = \mathbf{0}$$
$$\mathbf{L}(\mathbf{z}_{n+\frac{1}{2}}) \nabla \mathcal{S}(\mathbf{z}_{n+\frac{1}{2}}) = \mathbf{0} \tag{103}$$

To see whether the fundamental balance laws are correctly reproduced in the discrete formulation, we proceed along the lines of the time-continuous formulation in Section 4.2. In particular, concerning the balance of energy, similar to (89), we consider

$$\nabla \mathcal{E}(\mathbf{z}_{n+\frac{1}{2}}) \cdot (\mathbf{z}_{n+1} - \mathbf{z}_n)$$
$$= \Delta t \nabla \mathcal{E}(\mathbf{z}_{n+\frac{1}{2}}) \cdot \mathbf{L}(\mathbf{z}_{n+\frac{1}{2}}) \nabla \mathcal{E}(\mathbf{z}_{n+\frac{1}{2}}) + \Delta t \nabla \mathcal{E}(\mathbf{z}_{n+\frac{1}{2}}) \cdot \mathbf{M}(\mathbf{z}_{n+\frac{1}{2}}) \nabla \mathcal{S}(\mathbf{z}_{n+\frac{1}{2}}),$$

where (102) has been used. In analogy to the time-continuous case the right-hand side of the above equation vanishes due to the skew-symmetry of $\mathbf{L}(\mathbf{z}_{n+\frac{1}{2}})$ and non-interaction condition (103)$_1$. Thus

$$\nabla \mathcal{E}(\mathbf{z}_{n+\frac{1}{2}}) \cdot (\mathbf{z}_{n+1} - \mathbf{z}_n) = 0.$$

On the other side,

$$\nabla \mathcal{E}(\mathbf{z}_{n+\frac{1}{2}}) \cdot (\mathbf{z}_{n+1} - \mathbf{z}_n) \neq \mathcal{E}(\mathbf{z}_{n+1}) - \mathcal{E}(\mathbf{z}_n) \tag{104}$$

in general. This inequality complies with the well-known fact that the mid-point rule is not capable to conserve non-linear first integrals in general. However, there exists the exceptional case related to the choice $\tau = u$, for which (104) turns into an equality. This is due to the fact that for $\tau = u$ the total energy takes the form (96) and thus $\hat{\mathcal{E}}(\mathbf{z})$ is merely quadratic. Since the mid-point rule preserves quadratic first integrals (see Leimkuhler,[1] Sec. 4.4.2), the choice $\tau = u$ yields a structure-preserving scheme which is capable to conserve total energy.

Concerning the evolution of total entropy, guided by (91), we consider

$$\nabla S(\mathbf{z}_{n+\frac{1}{2}}) \cdot (\mathbf{z}_{n+1} - \mathbf{z}_n)$$

$$= \Delta t \nabla S(\mathbf{z}_{n+\frac{1}{2}}) \cdot \mathbf{L}(\mathbf{z}_{n+\frac{1}{2}}) \nabla \mathcal{E}(\mathbf{z}_{n+\frac{1}{2}}) + \Delta t \nabla S(\mathbf{z}_{n+\frac{1}{2}}) \cdot \mathbf{M}(\mathbf{z}_{n+\frac{1}{2}}) \nabla S(\mathbf{z}_{n+\frac{1}{2}}),$$

where again (102) has been used. Employing non-interaction condition $(103)_2$, we obtain

$$\nabla S(\mathbf{z}_{n+\frac{1}{2}}) \cdot (\mathbf{z}_{n+1} - \mathbf{z}_n) = \Delta t \nabla S(\mathbf{z}_{n+\frac{1}{2}}) \cdot \mathbf{M}(\mathbf{z}_{n+\frac{1}{2}}) \nabla S(\mathbf{z}_{n+\frac{1}{2}}) \geq 0, \tag{105}$$

where the positive semi-definiteness of friction matrix $\mathbf{M}(\mathbf{z}_{n+\frac{1}{2}})$ has been taken as a basis. On the other hand, in analogy to (104), we have

$$\nabla S(\mathbf{z}_{n+\frac{1}{2}}) \cdot (\mathbf{z}_{n+1} - \mathbf{z}_n) \neq S(\mathbf{z}_{n+1}) - S(\mathbf{z}_n). \tag{106}$$

This implies that, despite the encouraging result (105), the mid-point scheme in general does not guarantee a non-decreasing entropy. However, there again is an exception related to the choice $\tau = \eta$. For this particular case, the total entropy takes the form (99) and thus $\tilde{S}(\mathbf{z})$ is merely linear. Accordingly, the choice $\tau = \eta$ turns inequality (106) into an equality and the entropy-based mid-point scheme is therefore capable to correctly reproduce the second law of thermodynamics in the discrete setting.

We eventually verify that all mid-point-based schemes under consideration are capable to conserve angular momentum. The incremental change of angular momentum (94) can be written in the form

$$\mathbf{J}_{n+1}^{h} - \mathbf{J}_n^{h} = \mathbf{q}_{a_{n+\frac{1}{2}}} \times \left(\mathbf{p}_{n+1}^a - \mathbf{p}_{n+1}^a \right) - \mathbf{p}_{n+\frac{1}{2}}^a \times \left(\mathbf{q}_{a_{n+1}} - \mathbf{q}_{a_n} \right). \tag{107}$$

Mid-point scheme (102) gives rise to

$$\mathbf{q}_{a_{n+1}} - \mathbf{q}_{a_n} = \Delta t M_{ab} \mathbf{p}_{n+\frac{1}{2}}^b,$$

$$\mathbf{p}_{n+1}^a - \mathbf{p}_{n+1}^a = \Delta t \left(-\partial_{\mathbf{q}_a} \mathcal{E}(\mathbf{z}_{n+\frac{1}{2}}) + \mathbf{l}_b^a(\mathbf{z}_{n+\frac{1}{2}}) \, \partial_{\tau_b} \mathcal{E}(\mathbf{z}_{n+\frac{1}{2}}) \right). \tag{108}$$

Inserting from (108) into (107) yields

$$\mathbf{J}_{n+1}^{h} - \mathbf{J}_n^{h} = \Delta t \mathbf{q}_{a_{n+\frac{1}{2}}} \times \left(-\partial_{\mathbf{q}_a} \mathcal{E}(\mathbf{z}_{n+\frac{1}{2}}) + \mathbf{l}_b^a(\mathbf{z}_{n+\frac{1}{2}}) \, \partial_{\tau_b} \mathcal{E}(\mathbf{z}_{n+\frac{1}{2}}) \right) - \Delta t M_{ab} \mathbf{p}_{n+\frac{1}{2}}^a \times \mathbf{p}_{n+\frac{1}{2}}^b. \tag{109}$$

Symmetry conditions (93) imply

$$\mathbf{0} = \mathbf{q}_{a_{n+\frac{1}{2}}} \times \partial_{\mathbf{q}_a} \mathcal{E}(\mathbf{z}_{n+\frac{1}{2}}),$$

$$\mathbf{0} = \mathbf{q}_{a_{n+\frac{1}{2}}} \times \mathbf{l}_b^a(\mathbf{z}_{n+\frac{1}{2}}). \tag{110}$$

Inserting from (110) into (109) and taking into account the symmetry of M_{ab} together with the skew-symmetry of the vector product leads to the result $\mathbf{J}_{n+1}^{h} = \mathbf{J}_n^{h}$.

To summarize, depending on the choice for the thermodynamic variable we get three alternative mid-point schemes which are partially structure-preserving. Correspondingly, the resulting schemes are denoted by $(EM)_u$ (EM scheme related to $\tau = u$), $(ME)_\eta$ (momentum-entropy scheme associated with $\tau = \eta$), and M_θ (momentum scheme related to $\tau = \theta$).

5.2 | Fully structure-preserving schemes

In this section, we show that one specific modification of the three alternative mid-point-based schemes considered above turns all of them into EME schemes. That is, independent of the choice of $\tau \in \{\theta, \eta, u\}$, all scheme are (i) thermodynamically consistent in the sense that they obey discrete versions of the two fundamental laws of thermodynamics, and (ii) capable to conserve angular momentum.

To reach this goal, the aforementioned modification of the mid-point integrator should (i) maintain the structure-preserving properties (103), and (ii) ensure that inequalities (104) and (106) are turned into equalities for general nonlinear functions $\mathcal{E}(\mathbf{z})$ and $\mathcal{S}(\mathbf{z})$. For that purpose, we resort to the notion of discrete derivative introduced in Gonzalez.[41] In particular, we replace the mid-point derivatives $\nabla\mathcal{E}(\mathbf{z}_{n+\frac{1}{2}})$ and $\nabla\mathcal{S}(\mathbf{z}_{n+\frac{1}{2}})$ by discrete derivatives $d\mathcal{E}(\mathbf{z}_n, \mathbf{z}_{n+1})$ and $d\mathcal{S}(\mathbf{z}_n, \mathbf{z}_{n+1})$, respectively. Accordingly, starting with the discrete derivatives of the total energy, based on (74), we introduce the discrete derivatives

$$d_{\mathbf{q}_a}\mathcal{E} = \sum_{g=1}^{G}\left[d_{\mathbf{F}}u_g\nabla N^a(\mathbf{X}_g) - N^a(\mathbf{X}_g)\mathbf{b}(\mathbf{X}_g)\right]w_g,$$

$$d_{\mathbf{p}^a}\mathcal{E} = M_{ab}\mathbf{p}^b_{n+\frac{1}{2}},$$

$$d_{\tau_a}\mathcal{E} = \sum_{g=1}^{G}N^a(\mathbf{X}_g)d_{\tau}u_g w_g,$$

$$\frac{d\mathcal{E}}{d(\mathbf{C}_p^{-1})_g^{AB}} = w_g\frac{du_g}{d(\mathbf{C}_p^{-1})^{AB}}. \tag{111}$$

where the discrete derivatives of the internal energy density function $u(\mathbf{F}, \tau, \mathbf{C}_p^{-1})$ are denoted by $du/d(\mathbf{C}_p^{-1})^{AB}$, $d_{\tau}u$, and

$$d_{\mathbf{F}}u = 2\mathbf{F}_{n+\frac{1}{2}}d_{\mathbf{C}}u, \tag{112}$$

respectively. In the last equation, the frame-indifferent representation of the internal energy density has been accounted for (see Appendix A). We refer to Appendix B for the specific definitions of the discrete derivatives $d_{\mathbf{C}}u$, $d_{\tau}u$, and $du/d(\mathbf{C}_p^{-1})^{AB}$, respectively.

Similarly, the discrete derivatives of the total entropy rely on the application of the discrete derivative to the internal entropy density. That is, based on (76), we introduce

$$d_{\mathbf{q}_a}\mathcal{S} = \sum_{g=1}^{G}d_{\mathbf{F}}\eta_g\nabla N^a(\mathbf{X}_g)w_g,$$

$$d_{\mathbf{p}^a}\mathcal{S} = \mathbf{0},$$

$$d_{\tau_a}\mathcal{S} = \sum_{g=1}^{G}N^a(\mathbf{X}_g)d_{\tau}\eta_g w_g,$$

$$\frac{d\mathcal{S}}{d(\mathbf{C}_p^{-1})_g^{AB}} = w_g\frac{d\eta_g}{d(\mathbf{C}_p^{-1})^{AB}}. \tag{113}$$

where the discrete derivatives of the internal entropy density function $\eta(\mathbf{F}, \tau, \mathbf{C}_p^{-1})$ are denoted by $d\eta/d(\mathbf{C}_p^{-1})^{AB}$, $d_{\tau}\eta$, and

$$d_{\mathbf{F}}\eta = 2\mathbf{F}_{n+\frac{1}{2}}d_{\mathbf{C}}\eta, \tag{114}$$

respectively (see Appendix B for further details). In addition to (111) and (113), the derivatives of u and η contained in Poisson matrix (86) and friction matrix (88) need to be replaced by the corresponding discrete derivatives. The thus obtained discrete versions of the Poisson and friction matrix are denoted by $\mathbf{L}(\mathbf{z}_n, \mathbf{z}_{n+1})$ and $\mathbf{M}(\mathbf{z}_n, \mathbf{z}_{n+1})$, respectively. These modifications to mid-point integrator (102) yield fully structure-preserving EME schemes of the form

$$\mathbf{z}_{n+1} - \mathbf{z}_n = \Delta t\mathbf{L}(\mathbf{z}_n, \mathbf{z}_{n+1})d\mathcal{E}(\mathbf{z}_n, \mathbf{z}_{n+1}) + \Delta t\mathbf{M}(\mathbf{z}_n, \mathbf{z}_{n+1})d\mathcal{S}(\mathbf{z}_n, \mathbf{z}_{n+1}). \tag{115}$$

It is important to note that the above-described modifications of the mid-point rule retain the crucial non-interaction and symmetry conditions. In particular, non-interaction conditions (103) are now replaced by

$$M(\mathbf{z}_n, \mathbf{z}_{n+1})d\mathcal{E}(\mathbf{z}_n, \mathbf{z}_{n+1}) = \mathbf{0},$$
$$L(\mathbf{z}_n, \mathbf{z}_{n+1})d\mathcal{S}(\mathbf{z}_n, \mathbf{z}_{n+1}) = \mathbf{0}, \tag{116}$$

while symmetry conditions (110) are replaced by

$$0 = \mathbf{q}_{a_{n+\frac{1}{2}}} \times d_{\mathbf{q}_a} \mathcal{E}(\mathbf{z}_n, \mathbf{z}_{n+1}),$$

$$0 = \mathbf{q}_{a_{n+\frac{1}{2}}} \times \mathbf{l}_b^a(\mathbf{z}_n, \mathbf{z}_{n+1}). \tag{117}$$

Note that $\mathbf{l}_b^a$ has been introduced in $(85)_1$. Accordingly, following the present procedure, the discrete derivatives $d_{\mathbf{F}}\eta$ and $d_\tau\eta$ are used in $(85)_1$, to get $\mathbf{l}_b^a(\mathbf{z}_n, \mathbf{z}_{n+1})$.

The so-called directionality property of the (partitioned) discrete derivatives (cf. Gonzalez[41]) ensures that inequalities (104) and (106) are now replaced by the equalities

$$d\mathcal{E}(\mathbf{z}_n, \mathbf{z}_{n+1}) \cdot (\mathbf{z}_{n+1} - \mathbf{z}_n) = \mathcal{E}(\mathbf{z}_{n+1}) - \mathcal{E}(\mathbf{z}_n),$$

$$d\mathcal{S}(\mathbf{z}_n, \mathbf{z}_{n+1}) \cdot (\mathbf{z}_{n+1} - \mathbf{z}_n) = \mathcal{S}(\mathbf{z}_{n+1}) - \mathcal{S}(\mathbf{z}_n). \tag{118}$$

Note that directionality properties (118) are also verified in Appendix B.

The new schemes are indeed fully structure-preserving, independent of the choice for $\tau \in \{\theta, \eta, u\}$. This can be shown in a straightforward manner by following the steps in Section 5.1. For obvious reasons, the new EME consistent schemes are abbreviated with $(EME)_\theta$, $(EME)_\eta$, and $(EME)_u$.

6 | NUMERICAL INVESTIGATIONS

In this section, the alternative mid-point type schemes newly developed in the present work are applied to representative numerical examples dealing with finite strain thermo-viscoelastodynamics. Depending on the specific choice for the thermodynamic variable $\tau \in \{\theta, \eta, u\}$, the following methods are applied:

Variable	$\tau = u$	$\tau = \eta$	$\tau = \theta$
Section 5.1	$(EM)_u$	$(ME)_\eta$	$(M)_\theta$
Section 5.2	$(EME)_u$	$(EME)_\eta$	$(EME)_\theta$

In the numerical investigations, we shall focus on momentum maps associated with symmetries of the mechanical system at hand, and the balance laws associated with the two fundamental laws of thermodynamics. In this connection, we also consider the functional

$$\mathcal{L} = \mathcal{E} - \theta_0 \mathcal{S}. \tag{119}$$

According to Gurtin,[48] for certain types of environments, $\mathcal{L}$ is a natural Lyapunov function and thus qualifies as estimate for the numerical stability of the schemes under consideration.

In each time step, the schemes emanating from (102) and (115) generate a system of nonlinear algebraic equations for the determination of the state variables $\mathbf{z}_{n+1}$. To this end, we apply a Multilevel-Newton algorithm;[†] see Hartmann[49] and references therein for more details.

6.1 | Material model

In order to particularize the Helmholtz free energy density (28) used in the numerical examples, we start from a temperature-based description. In particular, we consider

$$\overline{\psi}(\mathbf{C}, \theta, \mathbf{C}_p^{-1}) = \overline{\psi}^{eq}(\mathbf{C}, \theta) + \overline{\psi}^{neq}(\mathbf{C}, \theta, \mathbf{C}_p^{-1}),$$

$$\overline{\psi}^{eq}(\mathbf{C}, \theta) = \psi_1(\mathbf{C}) + \psi_2(\theta) - (\theta - \theta_0)\psi_3(J),$$

$$\overline{\psi}^{neq}(\mathbf{C}, \theta, \mathbf{C}_p^{-1}) = \psi_{1,visc}(\mathbf{C}, \mathbf{C}_p^{-1}), \tag{120}$$

[†]In the numerical examples the local Newton tolerance refers to the solution of the material evolution equations while the global Newton tolerance refers to the solution of the whole system, cf. Tables 1 and 2.

where

$$\psi_1(\mathbf{C}) = \frac{\mu}{2}\left(\mathbf{C} : \mathbf{I} - 3 - 2\log J - \frac{2}{3}(J-1)^2\right) + W_{\text{vol}}(J),$$

$$\psi_{1,\text{visc}}(\mathbf{C}, \mathbf{C}_p^{-1}) = \frac{\mu_e}{2}\left(\mathbf{C} : \mathbf{C}_p^{-1} - 3 - 2\log J_e - \frac{2}{3}(J_e-1)^2\right) + W_{\text{vol,visc}}(J_e),$$

$$\psi_2(\theta) = c\left(\theta - \theta_0 - \theta\log(\theta/\theta_0)\right),$$

$$\psi_3(J) = 3\beta W_{\text{vol}}(J),$$

$$W_{\text{vol}}(J) = \frac{\lambda + \frac{2}{3}\mu}{4}\left((\log J)^2 + (J-1)^2\right),$$

$$W_{\text{vol,visc}}(J_e) = \frac{\lambda_e + \frac{2}{3}\mu_e}{4}\left((\log J_e)^2 + (J_e-1)^2\right). \tag{121}$$

Here, $J = \sqrt{\det \mathbf{C}}$ is the determinant of the deformation gradient, $J_e = \sqrt{\det(\mathbf{C}\mathbf{C}_p^{-1})}$ and μ, μ_e, λ, and λ_e are prescribed parameters, $c > 0$ is the specific heat capacity at constant deformation, β is the coefficient of thermal expansion, and θ_0 is the reference temperature. We refer to Betsch and Schiebl[39] and the references therein for a detailed investigation of the thermoelastic part of the specific Helmholtz free energy density (120). Further, for the viscoelastic part, we refer to Groß[15] and the references therein. For simplicity, we assume incompressible material behavior. Quasi-incompressible material models for finite strain thermo-viscoelasticy are considered in, for example, References 50 and 51. It is now a straightforward exercise to calculate further quantities emanating from (120), depending on the specific choice for the thermodynamic variable $\tau \in \{u, \theta, \eta\}$ (see also Betsch and Schiebl[39] for additional details). In particular, the *temperature-based formulation* yields

$$\overline{\eta}(\mathbf{C}, \theta, \mathbf{C}_p^{-1}) = c\log(\theta/\theta_0) + \psi_3(J),$$

$$\overline{u}(\mathbf{C}, \theta, \mathbf{C}_p^{-1}) = \psi_1(\mathbf{C}) + \psi_{1,\text{visc}}(\mathbf{C}, \mathbf{C}_p^{-1}) + c(\theta - \theta_0) + \theta_0\psi_3(J).$$

The formulation based on the *entropy density* gives

$$\tilde{\eta}(\mathbf{C}, \eta, \mathbf{C}_p^{-1}) = \eta,$$

$$\tilde{u}(\mathbf{C}, \eta, \mathbf{C}_p^{-1}) = \psi_1(\mathbf{C}) + \psi_{1,\text{visc}}(\mathbf{C}, \mathbf{C}_p^{-1}) + c\left(\theta_0 e^{\frac{\eta-\psi_3(J)}{c}} - \theta_0\right) + \theta_0\psi_3(J).$$

Moreover, the formulation based on the *internal energy density* leads to

$$\hat{\eta}(\mathbf{C}, u, \mathbf{C}_p^{-1}) = c\log\left(1 + \frac{u - \psi_1(\mathbf{C}) - \psi_{1,\text{visc}}(\mathbf{C}, \mathbf{C}_p^{-1})}{c\theta_0} - \frac{\psi_3(J)}{c}\right) + \psi_3(J),$$

$$\hat{u}(\mathbf{C}, u, \mathbf{C}_p^{-1}) = u.$$

Concerning the constitutive equation for the material heat flux vector, we assume thermally isotropic material, with material conductivity tensor given by

$$\mathbf{K} = kJ\mathbf{C}^{-1}. \tag{122}$$

Here, k is a prescribed coefficient of thermal conductivity and, as before, $J = \sqrt{\det(\mathbf{C})}$. Finally, the constitutive equation for the isotropic fourth-order material inelastic flow tensor is given by (see Groß and Betsch[12] or Reese and Govindjee[43] and references therein for the spatial representation of the isotropic fourth-order inelastic flow tensor)

$$\mathcal{N} = \frac{1}{2\nu_D}\left(\left[\mathbf{C}^{-1} \odot \mathbf{I}\right]\mathbf{C} - \frac{1}{3}\mathbf{I} \otimes \mathbf{I}\right) + \frac{1}{9\nu_V}\mathbf{I} \otimes \mathbf{I}, \tag{123}$$

where $\nu_D > 0$ and $\nu_V > 0$ represent the deviatoric and volumetric viscosities, respectively, and where $(\mathbf{A} \odot \mathbf{B})_{.B..}^{A\cdot CD} = \frac{1}{2}\left[(\mathbf{A})_{..}^{AC}(\mathbf{B})_{B.}^{.D} + (\mathbf{A})_{..}^{AD}(\mathbf{B})_{B.}^{.C}\right].$

6.2 | Flying L-shaped block

The first numerical example deals with the L-shaped block depicted in Figure 4.

The spatial discretization of the block relies on 117 tri-linear finite elements leading to 224 nodes. The initial temperature field is varying linearly over the height (x_3 direction) of the block. In particular, at $x_3 = 0$, the initial temperature is prescribed as θ_a, while at $x_3 = h$, the temperature is prescribed as θ_b. The whole block is assumed to be thermally insulated ($\bar{q} = 0$ on $\partial_q \mathcal{B} = \partial \mathcal{B}$). Starting at rest, Piola traction vectors $\bar{\mathbf{t}}_a$ and $\bar{\mathbf{t}}_b$ are acting on two parts of the boundary surface of the block (Figure 4). The external loads are applied in the form of a hat function over time. In particular, the traction vectors are given by

$$\bar{\mathbf{t}}_a = -\bar{\mathbf{t}}_b = f(t) \begin{pmatrix} 256/9 \\ 512/9 \\ 768/9 \end{pmatrix} \text{Pa}, \quad f(t) = \begin{cases} t & \text{for} \quad 0\text{s} \leq t \leq 2\text{s} \\ 4 - t & \text{for} \quad 2\text{s} \leq t \leq 4\text{s} \\ 0 & \text{for} \quad t > 4\text{s}. \end{cases} \tag{124}$$

Table 1 provides a summary of the data used in the simulations. During the loading phase ($t \leq 4\text{s}$) the time step size for all simulations is $\Delta t = 0.05$, such that all systems start from the same energy- and entropy level directly after vanishing external loads. No Dirichlet boundary conditions are applied. Since in the initial loading phase the external forces are equilibrated, the total linear momentum of the block is a conserved quantity. In addition to that, after the loading phase ($t \geq 4\text{s}$) no external torque is acting on the block.

Consequently, the total angular momentum is conserved as well. All of the integrators under consideration are capable to exactly conserve both momentum maps (up to numerical round-off), independent of the chosen time step. This can be observed from Figure 5, where representative numerical results of the EM integrator $(EM)_u$ are shown. After the loading phase, the total energy must be a conserved quantity. As expected, the $(EM)_u$ scheme does exactly reproduce this conservation law (up to numerical round-off); see Figure 6. In contrary, the schemes $(M)_\theta$ and $(ME)_\eta$ are not capable of conserving the total energy for larger time step sizes. Depending on the time step size, both schemes tend to increase the energy which can be observed from Figure 7. Typically, such energy blow-ups eventually lead to a failure of the iterative (Newton-Raphson) solution procedure. In the diagrams, the break down of the simulation is indicated by vertical lines.

Regardless of the capability of the $(EM)_u$ scheme to conserve the total energy, the simulation still breaks down at about the same point in time as the break down of $(M)_\theta$ and $(ME)_\eta$ occurs. The numerical instability of $(EM)_u$ is accompanied by a nonphysical decrease of the total entropy as can be observed from Figure 8. Although not as pronounced as $(EM)_u$, $(M)_\theta$ occasionally yields an incremental decrease of the total entropy (Figure 8). However, the total entropy ought to be a non-decreasing function of time. In contrast to $(EM)_u$ and $(M)_\theta$, $(ME)_\eta$ is capable to correctly adhere to the second law of thermodynamics, independent of the time step (Figure 9). Indeed, in each time step, the total entropy does increase, as can be observed from Figure 9.
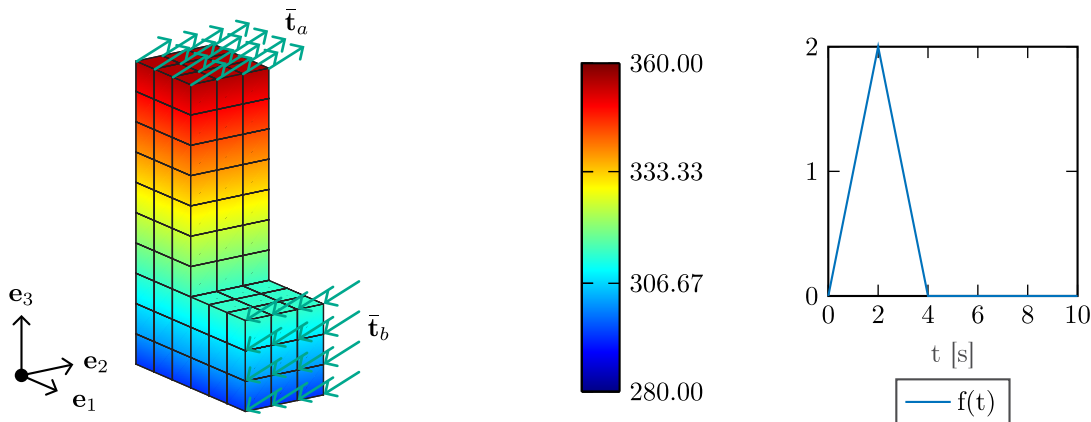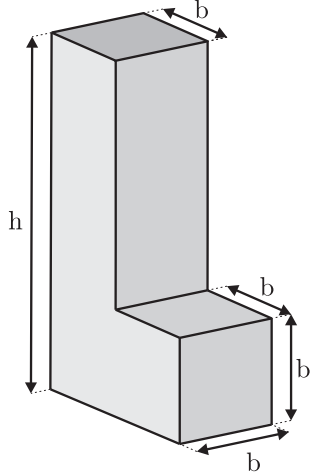

FIGURE 4 L-shaped block: Discretized block with initial temperature distribution and mechanical boundary conditions (left), load function over time (right)

TABLE 1 L-shaped block: Data used in the simulations

Lamé parameters	μ	997.5	Pa	Geometry
	λ	4544	Pa	
	μ_e	49.875	Pa	
	λ_e	272.2	Pa	
Specific heat capacity	c	100	$JK^{-1}m^{-3}$	
Expansion coefficient	β	$2.233 \cdot 10^{-4}$	K^{-1}	
Thermal conductivity	k	10	$WK^{-1}m^{-1}$	
Viscosities	ν_D	500	Jsm^{-3}	
	ν_V	100	Jsm^{-3}	
Ref. temperature	θ_0	293.15	K	
Mass density	ρ	100	kgm^{-3}	
Initial temperature	θ_a	290	K	
	θ_b	360	K	
Geometry	h	10	m	
	b	3	m	
Newton tolerance global	ε_g	10^{-8}	–	
Newton tolerance local	ε_l	10^{-9}	–	
Simulation duration	T	300	s	
Time step	Δt	0.05, 0.5, 0.6	s	
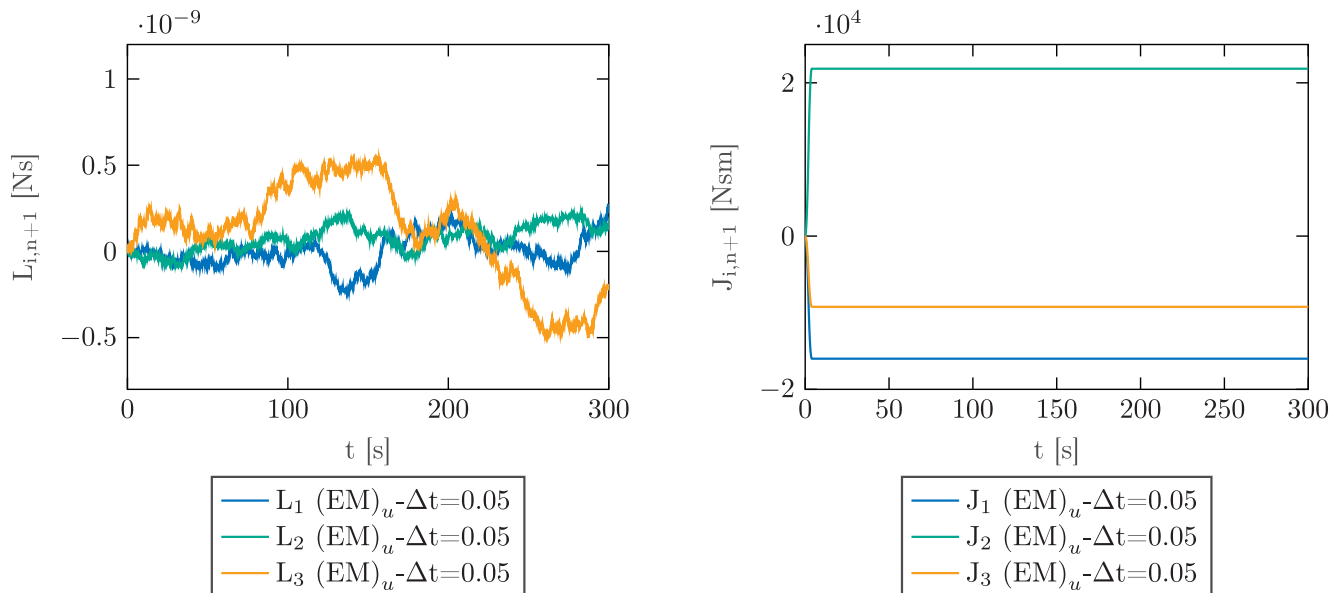
FIGURE 5 L-shaped block: Algorithmic conservation of linear momentum $(EM)_u$ scheme (left), Total discrete angular momentum $(EM)_u$ scheme (right)
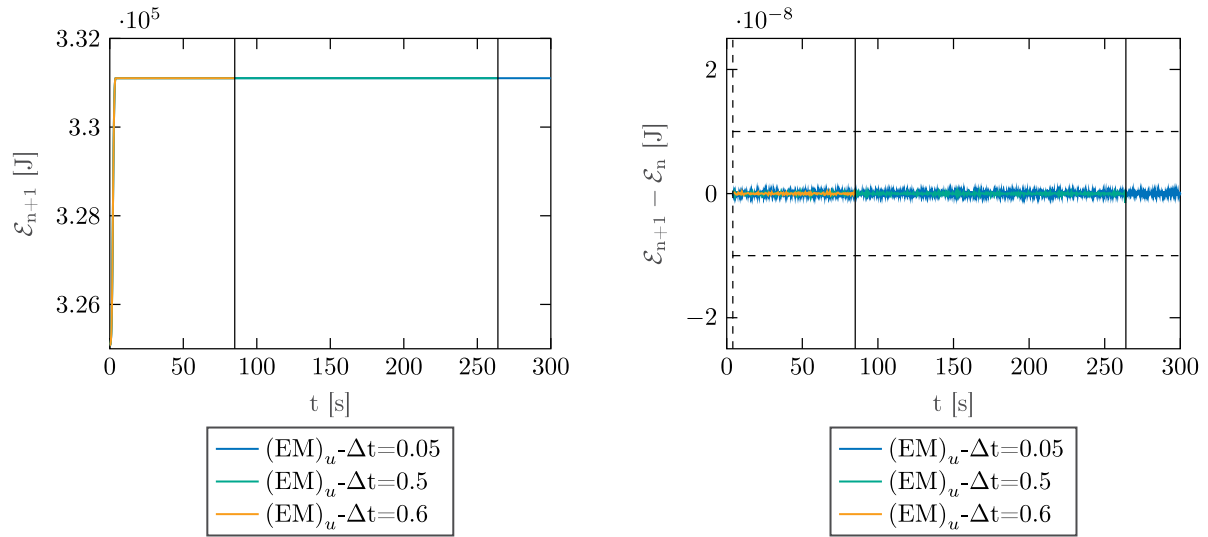
FIGURE 6 L-shaped block: Total energy $(EM)_u$ scheme (left), Incremental change of total energy $(EM)_u$ scheme (right)
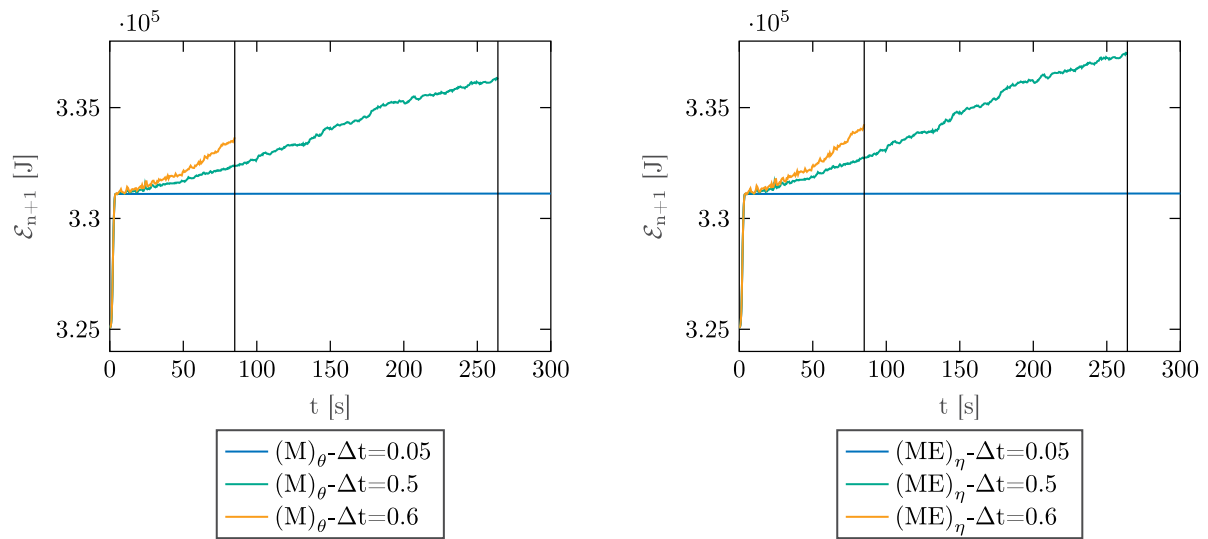
FIGURE 7 L-shaped block: Total energy $(M)_\theta$ scheme (left), Total energy $(ME)_\eta$ scheme (right)
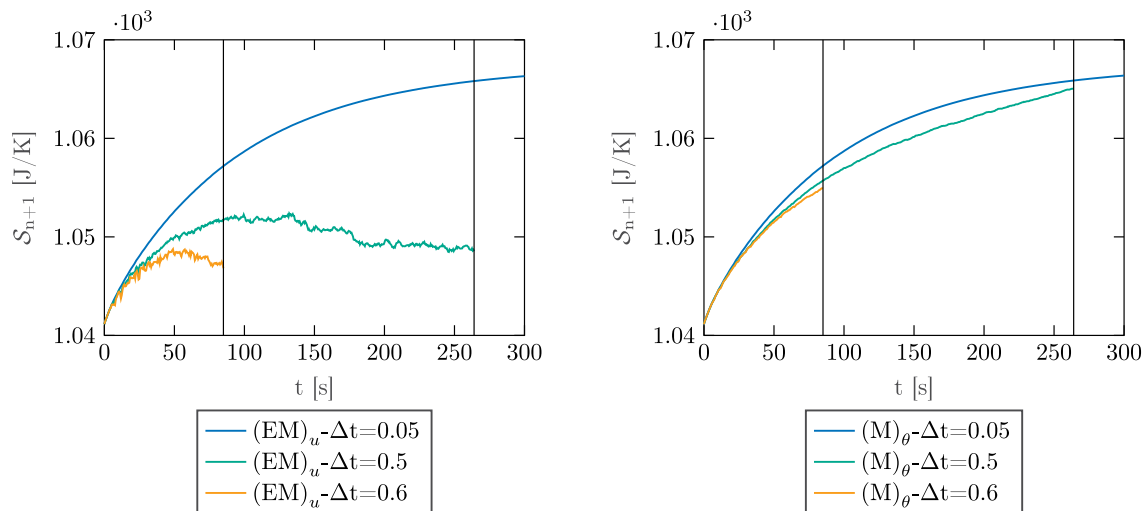
FIGURE 8 L-shaped block: Total entropy $(EM)_u$ scheme (left), Total entropy $(M)_\theta$ scheme (right)
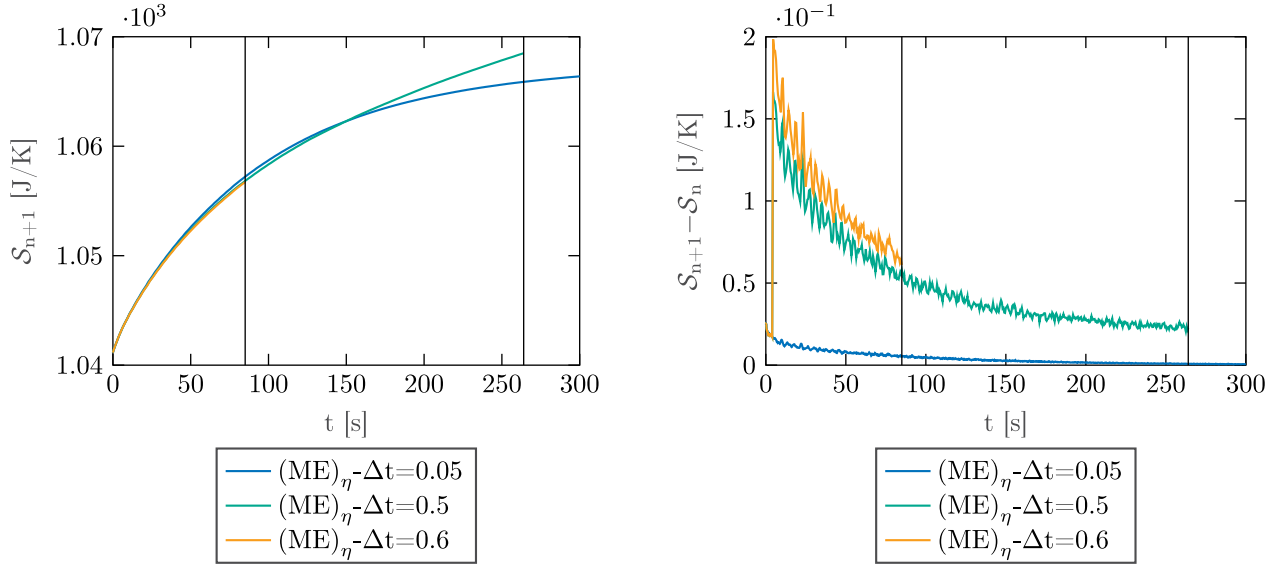
FIGURE 9 L-shaped block: total entropy $(ME)_\eta$ scheme (left), Incremental change of total entropy $(ME)_\eta$ scheme (right)

The incremental change of total entropy of the closed system at hand is related to heat conduction and inelastic deformations. For the mid-point rule, it can be directly calculated from (105). A straightforward calculation taking into account friction matrix (88) yields

$$
\mathcal{S}_{n+1} - \mathcal{S}_n \approx \Delta t \left(\sum_{g=1}^{G} \mathcal{D}^g_{\text{cond}} \Big|_{n+\frac{1}{2}} w_g + \mathcal{D}^g_{\text{inel}} \Big|_{n+\frac{1}{2}} w_g \right),
\tag{125}
$$

where

$$
\mathcal{D}^g_{\text{cond}} \Big|_{n+\frac{1}{2}} = (\Theta_{g_{n+\frac{1}{2}}})^2 \nabla \left(\frac{1}{\Theta_{g_{n+\frac{1}{2}}}} \right) \cdot \mathbf{K}_{g_{n+\frac{1}{2}}} \nabla \left(\frac{1}{\Theta_{g_{n+\frac{1}{2}}}} \right),
$$

$$
\mathcal{D}^g_{\text{inel}} \Big|_{n+\frac{1}{2}} = \frac{1}{\Theta_{g_{n+\frac{1}{2}}}} \mathbf{M}_{g_{n+\frac{1}{2}}} : \mathcal{N}_{g_{n+\frac{1}{2}}} : \mathbf{M}_{g_{n+\frac{1}{2}}}.
$$

Note that (125) can be viewed as discrete version of (25). Accordingly, for sufficiently small time steps, the incremental change of total entropy can be calculated for the mid-point schemes from (125). Similarly, for the EME schemes, the incremental change of total entropy can be calculated from (118)$_2$. The two contributions to the discrete evolution of the incremental change of total entropy are visualized in Figures 10 and 11.

After the loading phase, the environment of the present example can be characterized as thermally perfect in the sense of Gurtin.[48] Thus $\mathcal{L}$ defined in (119) plays the role of a Lyapunov function that has to decrease with time (Figure 12). However, the partially structure-preserving schemes $(EM)_u$, $(ME)_\eta$, and $(M)_\theta$ do not correctly reproduce this behavior, as can be seen from Figures 13 and 14. That is, depending on the time step and the duration of the simulation, all of the schemes inevitably exhibit numerical instabilities characterized by increasing values of $\mathcal{L}$.

Only the EME schemes developed in Section 5.2 completely reproduce the required behavior and thus can prevent numerical instabilities. This can be concluded from Figures 12 and 14, where the results of $(EME)_\eta$ are shown. The corresponding results of $(EME)_\theta$ and $(EME)_u$ are practically indistinguishable from those of $(EME)_\eta$.

Eventually, the motion of the L-shaped block is illustrated in Figure 15 with snapshots at successive points in time. In addition to that, the distribution of the temperature over the block is shown.
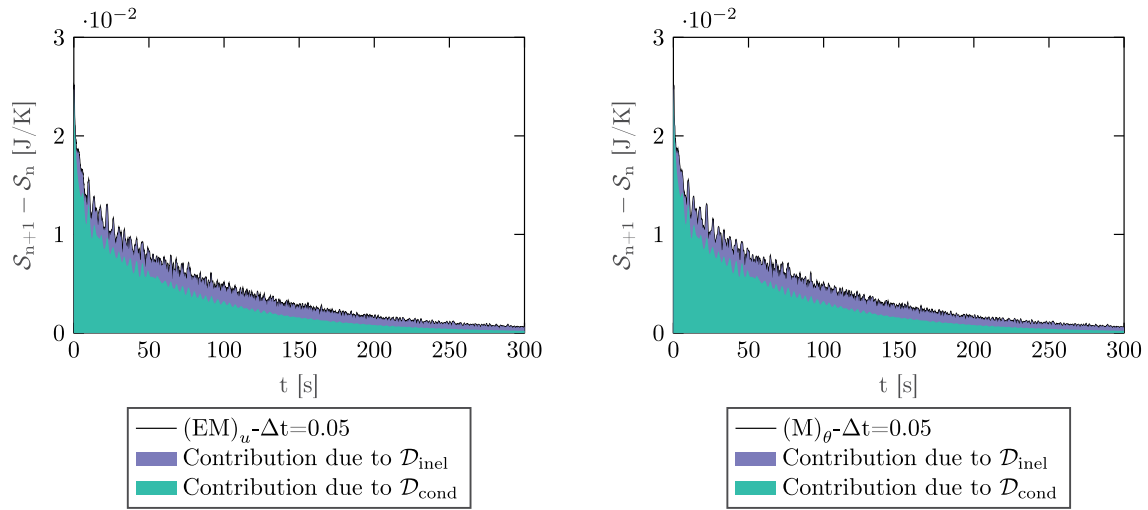
FIGURE 10   L-shaped block: Contributions to incremental change of entropy (EM)$_u$ scheme (left) and contributions to incremental change of entropy (M)$_\theta$ scheme (right)
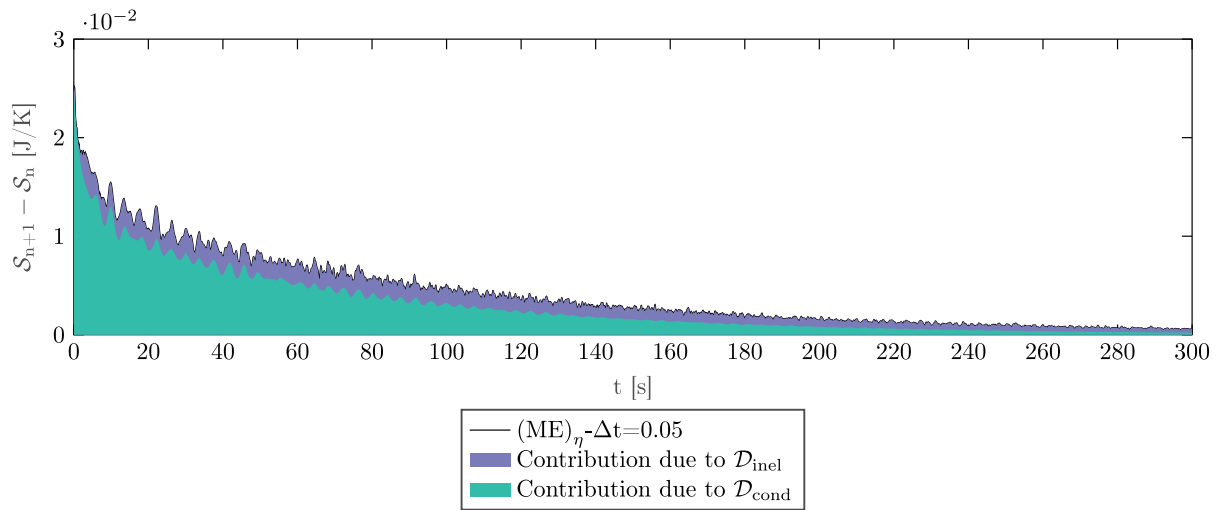

FIGURE 11   L-shaped block: Contributions to incremental change of entropy (ME)$_\eta$ scheme
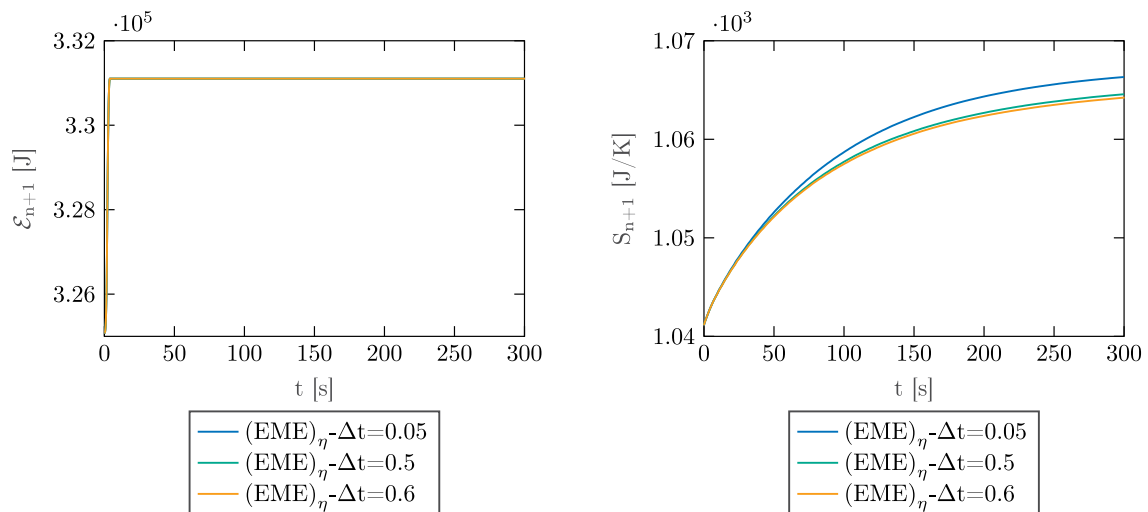

FIGURE 12   L-shaped block: Total energy (EME)$_\eta$ scheme (left) and total entropy (EME)$_\eta$ scheme (right)
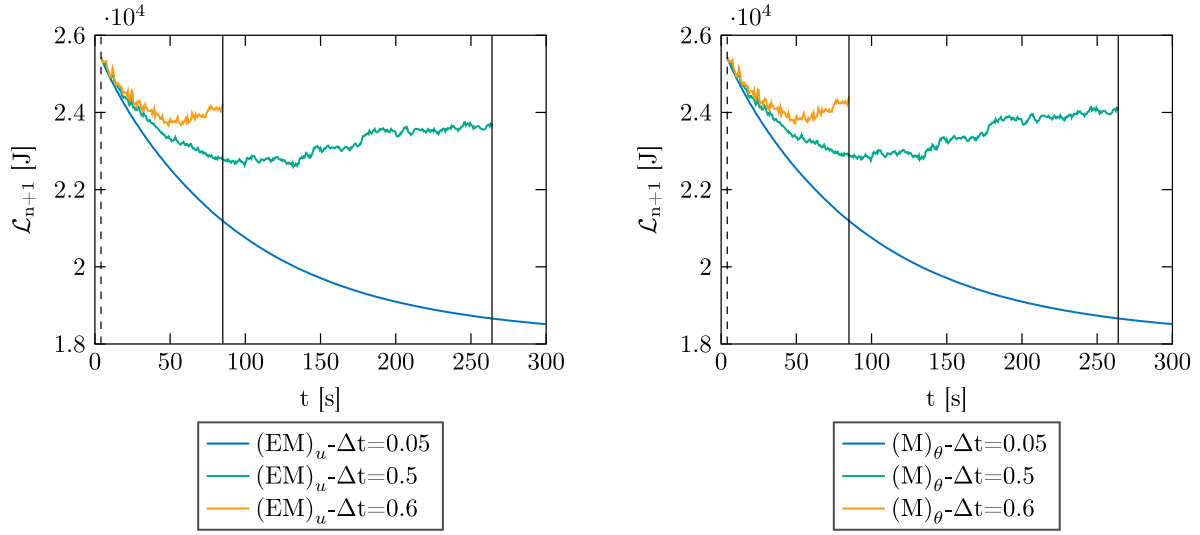
FIGURE 13 L-shaped block: Lyapunov function $(EM)_u$ scheme (left) and Lyapunov function $(M)_\theta$ scheme (right)
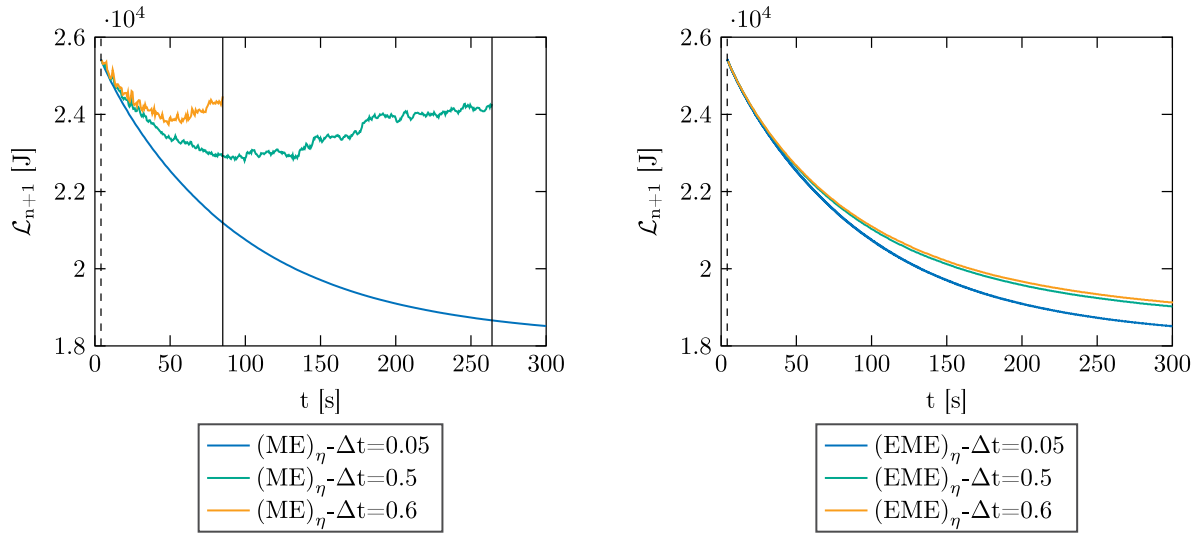
FIGURE 14 L-shaped block: Lyapunov function $(ME)_\eta$ scheme (left) and Lyapunov function $(EME)_\eta$ scheme (right)
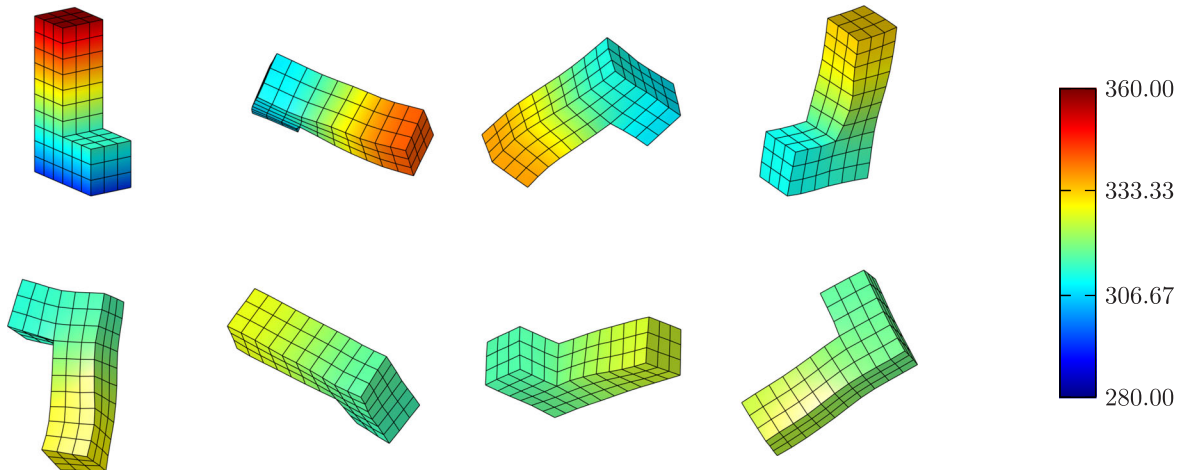
FIGURE 15 L-shaped block: Snapshots of the motion along with the temperature distribution over the block at $t \in \{0, 40, 80, 120, 160, 200, 240, 280\}$s, obtained with the $(EM)_u$ scheme and time step $\Delta t = 0.05$s
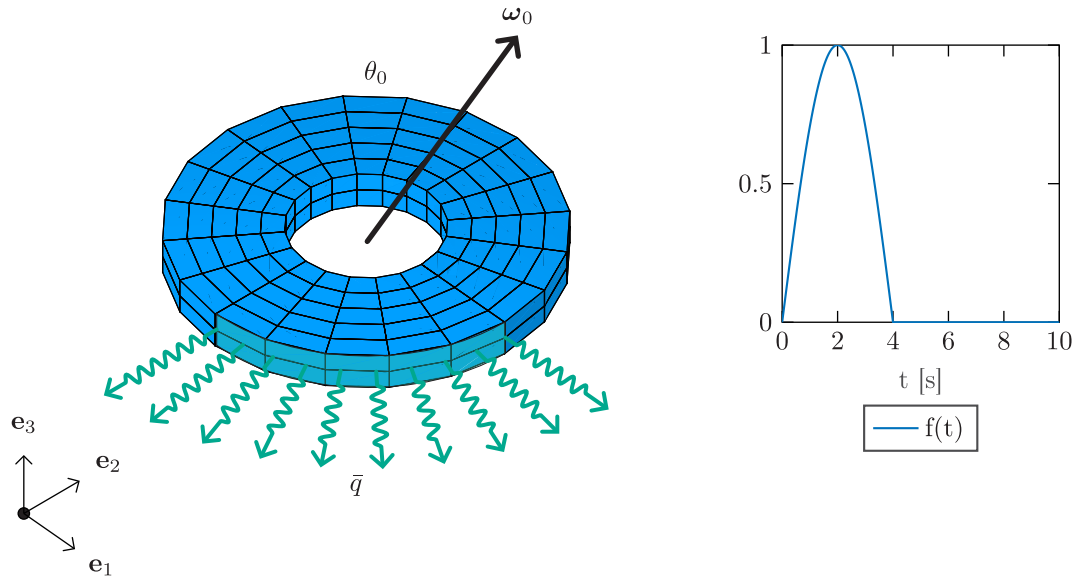
FIGURE 16   Rotating disk: Initial configuration and thermal boundary conditions (left) and function $f(t)$ for the prescribed heat flow over part of the boundary surface (right)

6.3 | Rotating disk

The second example deals with a rotating disk subjected to prescribed heat flow over part of the boundary surface (Figure 16). The spatial discretization of the disk is based on 200 tri-linear finite elements leading to a total of 360 nodes.

The initial velocity distribution over the disk results from a prescribed angular velocity $\boldsymbol{\omega}_0 \in \mathbb{R}^3$ and is given by
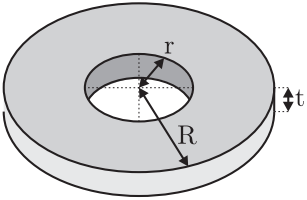
$$\mathbf{v}_0(\mathbf{X}) = \boldsymbol{\omega}_0 \times \mathbf{X}, \qquad \boldsymbol{\omega}_0 = \begin{pmatrix} 1 \\ 1 \\ 1 \end{pmatrix} \frac{1}{\mathrm{s}}.$$

The initial temperature of the disk is homogeneously distributed and equal to the reference temperature θ_0. In an initial period of time, $t \in [0, 4]$s, heat flow is prescribed over one quarter of the lateral boundary surface (Figure 16). In particular, the heat flow into the disk is described by

$$\bar{q} = -\frac{2000W}{\pi \mathrm{m}^2} f(t), \qquad f(t) = \begin{cases} \sin(\frac{\pi}{4\mathrm{s}}t) & \text{for} \quad 0 \leq t \leq 4\mathrm{s} \\ 0 & \text{for} \quad t > 4\mathrm{s}. \end{cases}$$

A plot of function $f(t)$ can be found in Figure 16. The rest of the boundary surface of the disk is assumed to be thermally insulated ($\bar{q} = 0$). Note that the prescribed heat flow vanishes after $t = 4$s. For $t > 4$s, the complete boundary surface of the disk is assumed to be thermally insulated ($\bar{q} = 0$ on $\partial_q \mathcal{B} = \partial \mathcal{B}$). Then the environment of the disk is thermally perfect in the sense of Gurtin.[48] A summary of the data used in the simulations of the rotating disk can be found in Table 2. During the loading phase ($t \leq 4$s) the time step size for all simulations is $\Delta t = 0.04$, such that all systems start from the same energy and entropy level directly after vanishing external loads. Due to the fact that neither external loads act on the disk, nor displacement boundary conditions are imposed, the mechanical system at hand has translational and rotational symmetry. Consequently, the corresponding momentum maps are first integrals of the motion. All integrators under consideration are capable to conserve the respective momentum map. Representative numerical results are shown in Figure 17.

TABLE 2 Rotating disk: Data used in the simulations

Material parameters	λ	3000	Pa	Geometry
	μ	750	Pa	
	μ_e	120	Pa	
	λ_e	37.5	Pa	
Specific heat capacity	c	150	$JK^{-1}m^{-3}$	
Expansion coefficient	β	$1 \cdot 10^{-4}$	K^{-1}	
Thermal conductivity	k	20	$WK^{-1}m^{-1}$	
Viscosities	ν_D	50	Jsm^{-3}	
	ν_V	10	Jsm^{-3}	
Ref. temperature	θ_0	293.15	K	
Mass density	ρ	8.93	kgm^{-3}	
Radius	r	0.8	m	
	R	2	m	
Thickness	t	0.4	m	
Newton tolerance global	ε_g	10^{-8}	–	
Newton tolerance local	ε_l	10^{-9}	–	
Simulation time	T	30	s	
Time step	Δt	0.04, 0.08, 0.1	s	

Since heat flow into the system is prescribed in the initial time period $[0, 4]$s, the total energy is expected to increase. For $t > 4$s, the system is closed and the total energy should stay constant. Again the $(EM)_u$ scheme is capable to correctly reproduce the first law (Figure 18).

However, despite the algorithmic energy conservation (for $t > 4$s), the $(EM)_u$ scheme is not devoid of numerical instabilities, depending on the time step. The corresponding point in time of the break down of the simulation is indicated with a vertical line in the diagrams. At about the same points in time, $(ME)_\eta$ and $(M)_\theta$ break down as well (Figure 19). For these schemes the break down is accompanied by a sudden increase of the total energy leading to the divergence of the Newton-Raphson iterations. For the considered duration of the simulation ($t \in [0, 30]$s), a time step of $\Delta t = 0.04$s is small enough to retain numerical stability of the three partially structure-preserving schemes at hand. The EME schemes developed in Section 5.2 do not lead to any numerical instabilities even for the large time step $\Delta t = 0.1$s. In particular, all of the EME schemes are capable to conserve the total energy for $t > 0.4$s. This is shown exemplarily for $(EME)_\eta$ in Figure 24.

Due to the prescribed heat flow into the disk, the total entropy of the disk is expected to increase in the initial time period $[0, 4]$s. For $t > 4$s, the system is closed and the total entropy should be a non-decreasing function of time. The $(EM)_u$ scheme does not correctly reproduce the second law as can be seen from Figure 20. Accordingly, the divergence of the iterative solution procedure is accompanied by a nonphysical decrease of the total entropy. The $(M)_\theta$ closely adheres to the second law as can be observed from Figure 20. As expected, the $(ME)_\eta$ scheme is capable to exactly satisfy the second law, independent of the time step. This can be observed from Figure 21. In particular, Figure 21(right) confirms that the change per time step of the total entropy is always positive. As expected all of the EME schemes are capable to correctly reproduce the non-decreasing evolution of the total entropy. This is shown exemplarily for $(EME)_\eta$ in Figure 24.

In addition, the two contributions to the discrete evolution of the incremental change of total entropy, see (125), are visualized in Figures 22 and 23 for the mid-point-based schemes. Most of the contribution is due to conduction of heat, only about 5.9% is due to inelastic deformations in the present example (Figure 24).

To shed further light on the numerical stability of the present schemes, we consider the Lyapunov function $\mathcal{L}$ defined in (119). For $t > 4$s the system is closed and the function $\mathcal{L}$ should decrease with time. As expected, the partially structure-preserving schemes $(EM)_u$, $(ME)_\eta$, and $(M)_\theta$ in general do not correctly reproduce this behavior, depending on
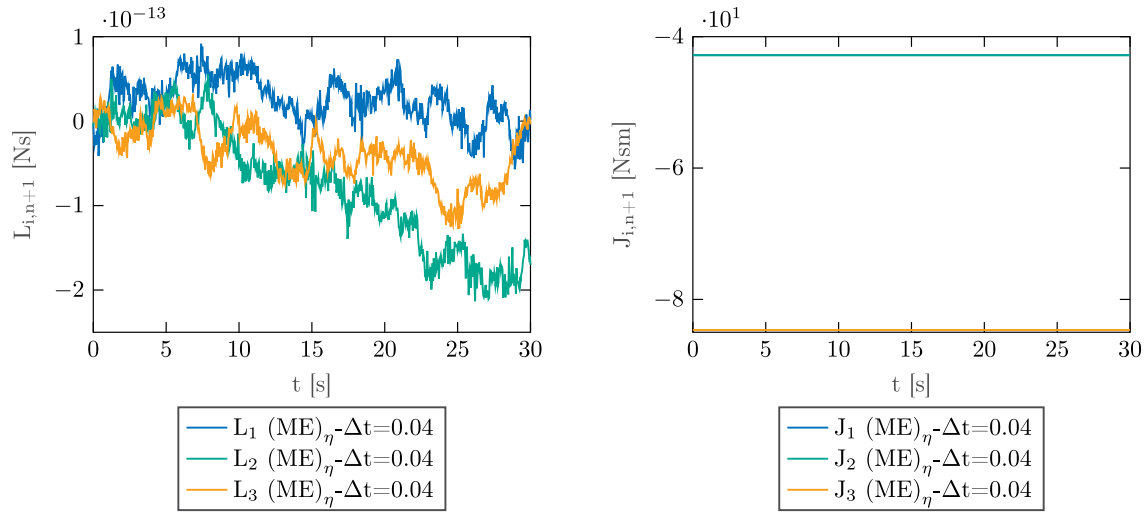
FIGURE 17 Rotating disk: Algorithmic conservation of linear momentum $(EM)_\eta$ scheme (left) and total discrete angular momentum $(EM)_\eta$ scheme (right)
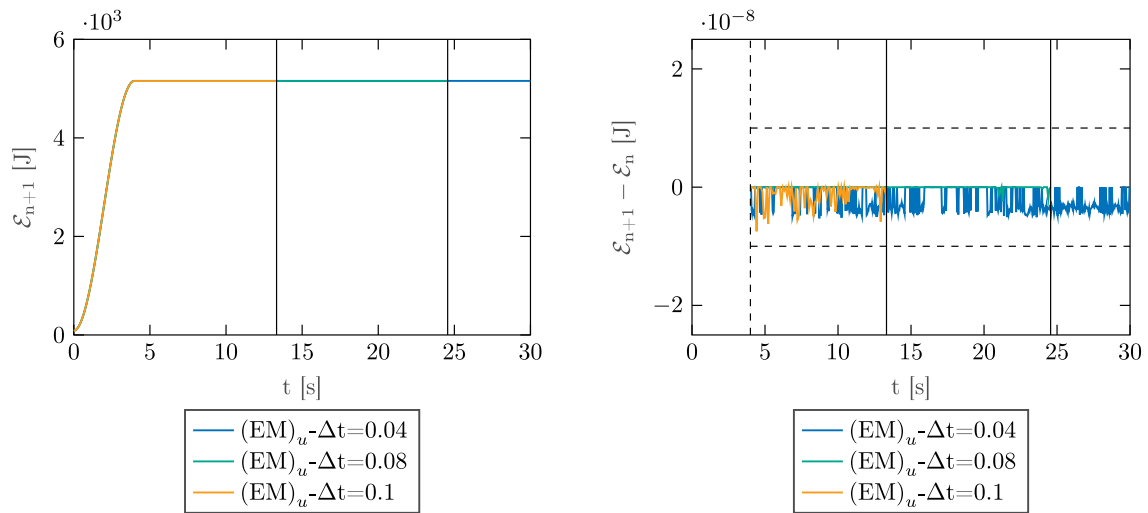

FIGURE 18 Rotating disk: Total energy $(EM)_u$ scheme (left) and incremental change of total energy $(EM)_u$ scheme (right)
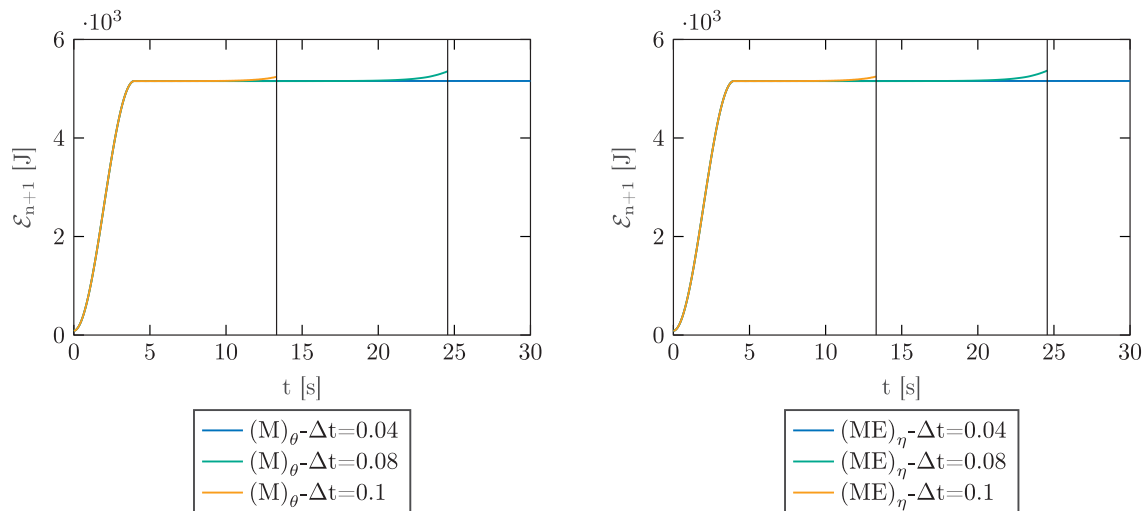

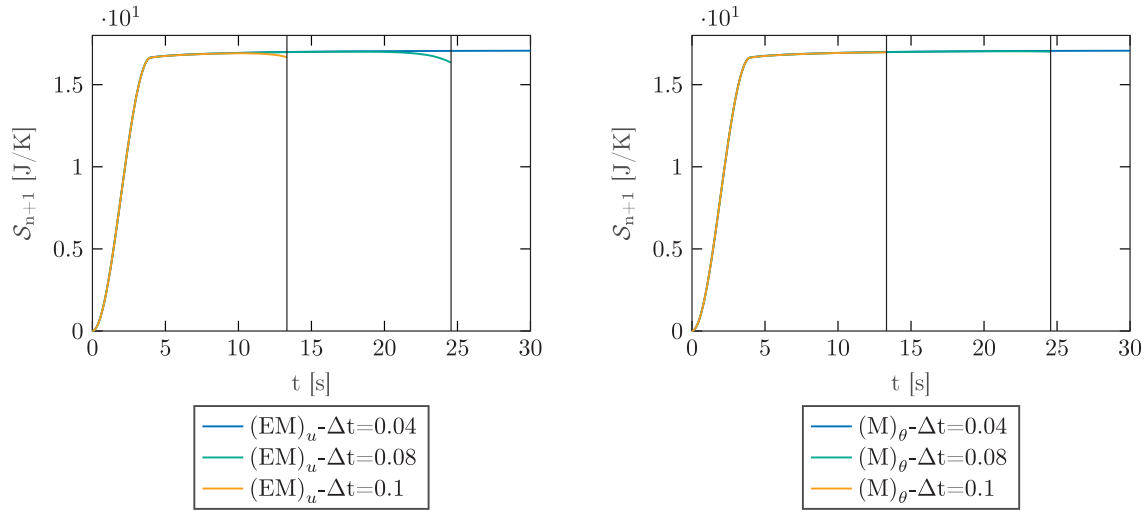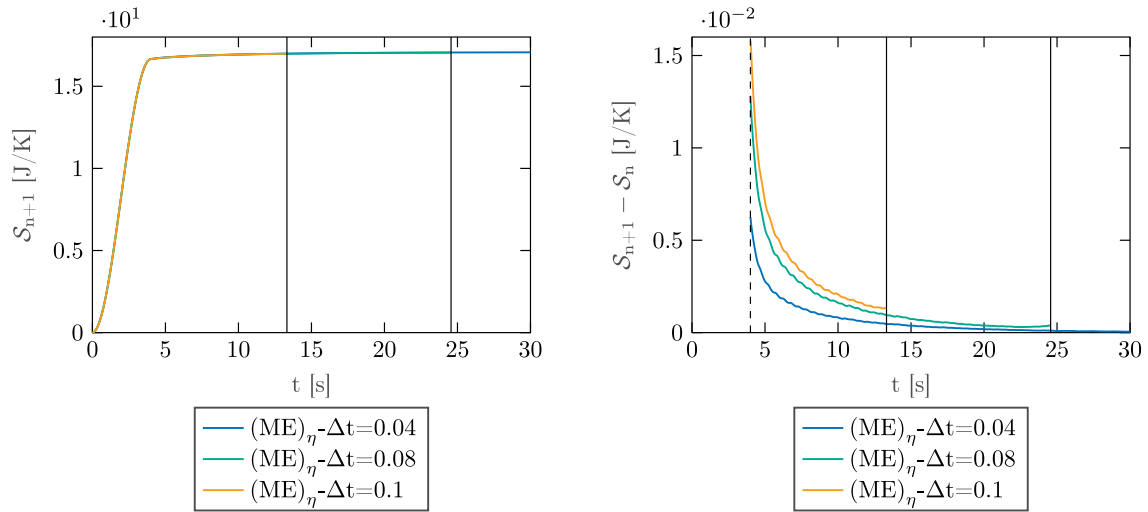**FIGURE 19** Rotating disk: Total energy $(M)_\theta$ scheme (left) and total energy $(ME)_\eta$ scheme (right)

FIGURE 20   Rotating disk: Total entropy $(EM)_u$ scheme (left) and total entropy $(M)_\theta$ scheme (right)

FIGURE 21   Rotating disk: Total entropy $(ME)_\eta$ scheme (left), and incremental change of total entropy $(ME)_\eta$ scheme (right)
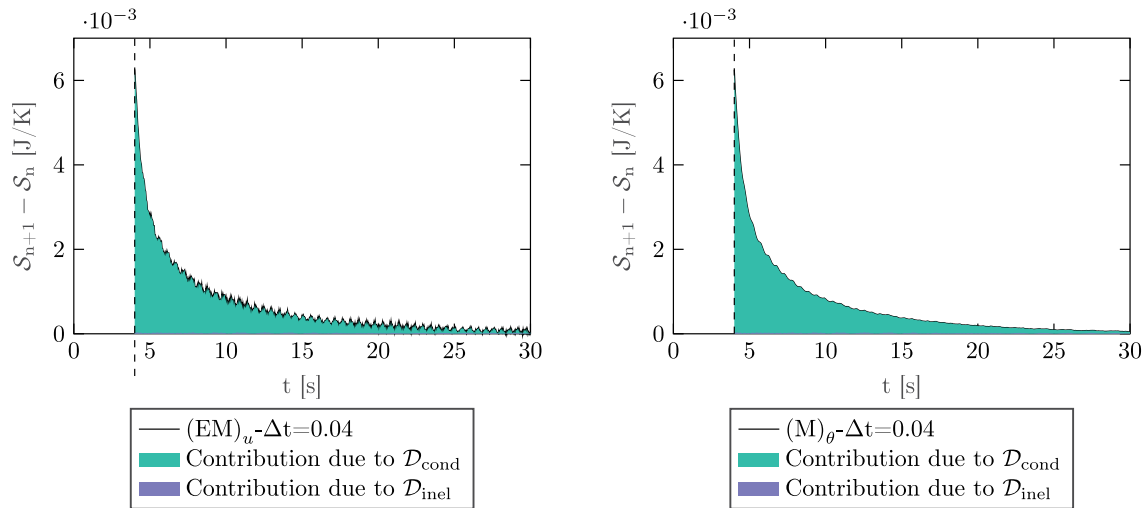

FIGURE 22   Rotating disk: Contributions to incremental change of entropy $(EM)_u$ scheme (left) and contributions to incremental change of entropy $(M)_\theta$ scheme (right)
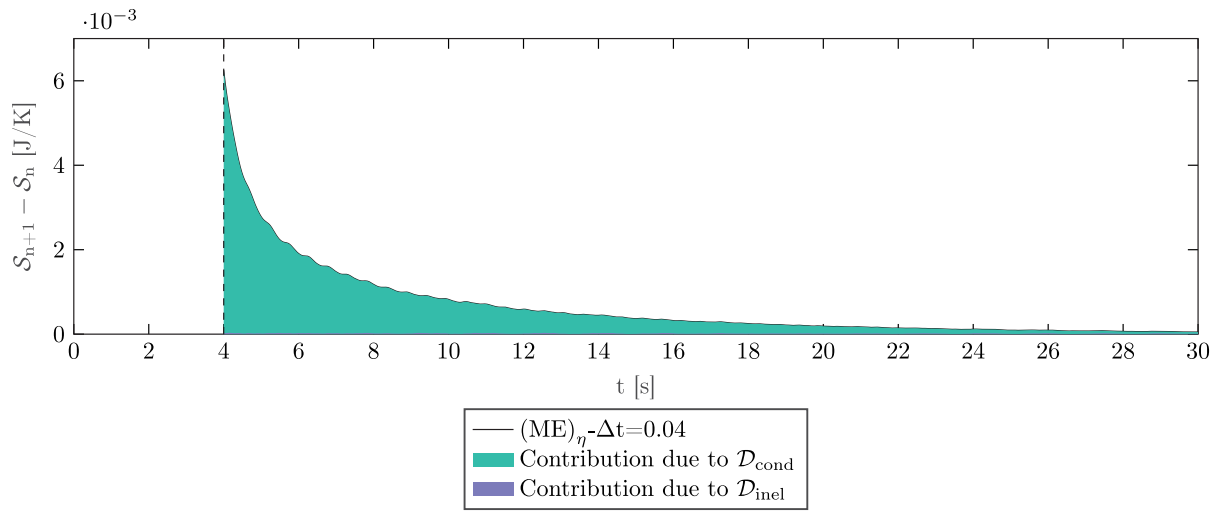
FIGURE 23 Rotating disk: Contributions to incremental change of entropy $(ME)_\eta$ scheme
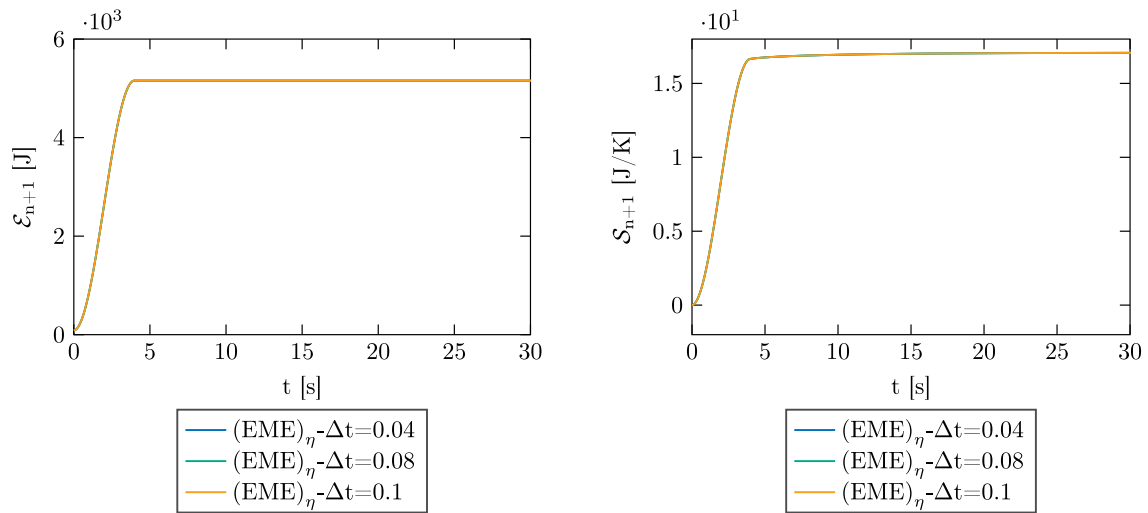

FIGURE 24 Rotating disk: Total energy $(EME)_\eta$ scheme (left), and total entropy $(EME)_\eta$ scheme (right)
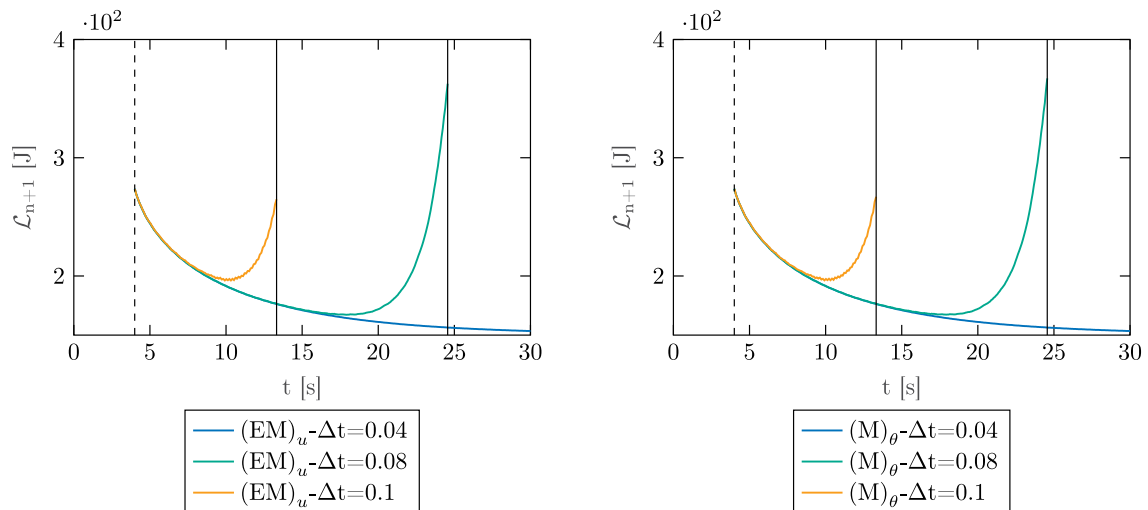

FIGURE 25 Rotating disk: Lyapunov function $(EM)_u$ scheme (left) and Lyapunov function $(M)_\theta$ scheme (right)
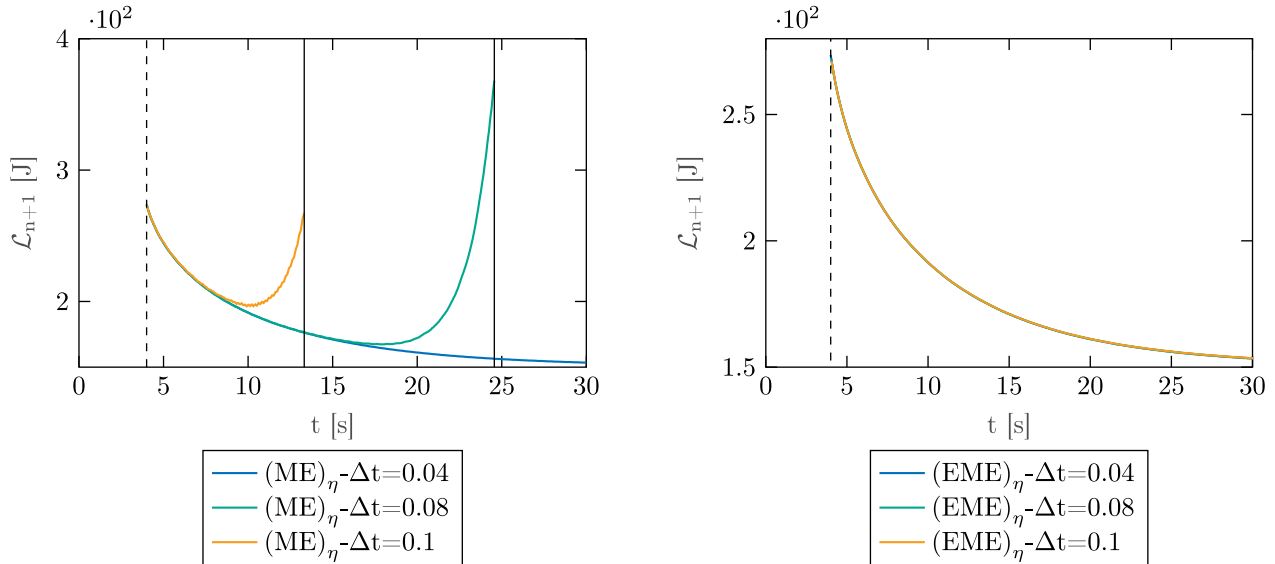
FIGURE 26 Rotating disk: Lyapunov function $(ME)_\eta$ scheme and Lyapunov function $(EME)_\eta$ scheme (right)
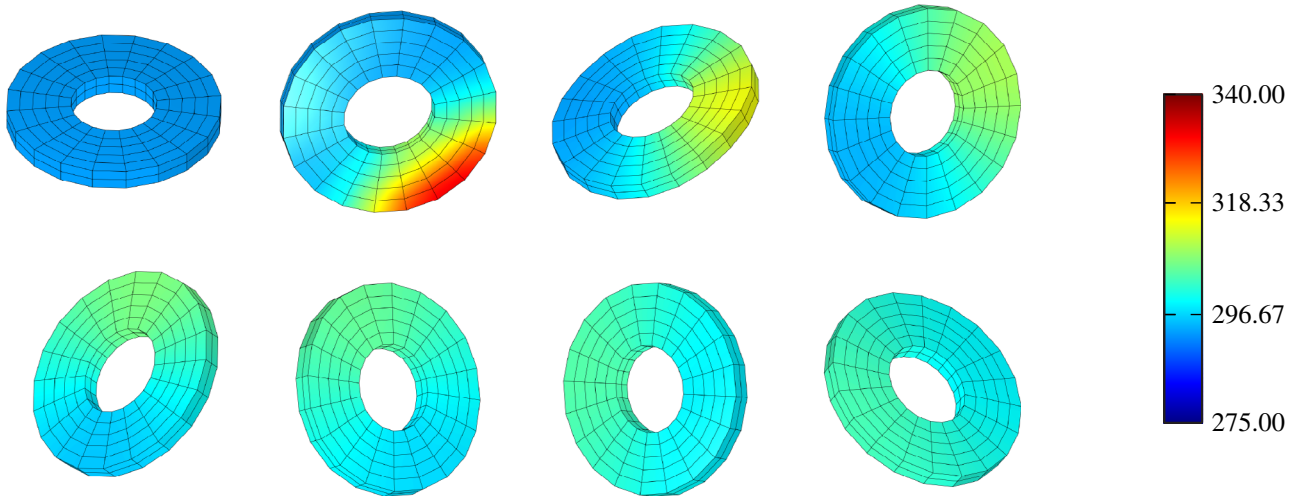

FIGURE 27 Rotating disk: Snapshots of the motion along with the temperature distribution over the block at $t \in \{0, 4, 8, 12, 16, 20, 24, 28\}$s, obtained with the $(ME)_\eta$ scheme and time step $\Delta t = 0.04$s

the size of the time step and the duration of the simulation (Figures 25 and 26). In particular, it can be seen that the smallest time step, $\Delta t = 0.04$s, yields a stable numerical simulation, at least in the considered time interval $[0, 30]$s. However, for larger time steps $\Delta t = 0.08$s and $\Delta t = 0.1$s, the numerical instability of each scheme becomes visible through the increase of $\mathcal{L}$. Again the fully structure-preserving EME schemes developed in Section 5.2 provide enhanced numerical stability. All of them lead to a steadily decreasing $\mathcal{L}$, independent of the time step size. This is shown exemplarily for EME in Figure 26.

Eventually, the motion of the disk is illustrated in Figure 27 with snapshots at successive points in time. In addition to that, the distribution of the temperature over the disk is shown.

7 | CONCLUSIONS

Starting from a GENERIC-based formulation of large-strain thermo-viscoelasticity, we have developed alternative structure-preserving schemes based on the implicit mid-point rule. Depending on the choice of the thermodynamic

variable, already the plain mid-point rule yields partially structure-preserving schemes (see Section 5.1). Despite this, these schemes cannot prevent from numerical instabilities as has been shown in the numerical examples. Specifically, choosing the internal energy density as thermodynamic variable leads to an EM scheme (called $(EM)_u$). For Hamiltonian mechanical systems, EM schemes typically provide enhanced numerical stability. However, this situation does no extend to thermomechanically coupled dissipative systems. Here, EME schemes such as those developed in Section 5.2 are required to prevent numerical instabilities.

The three EME schemes newly proposed in the present work essentially rely on the following features:

- The underlying GENERIC formulation in bracket form (Section 2) leads to characteristic expressions such as (14) and (17) for the first Piola-Kirchhoff stress tensor and the Mandel stress tensor, respectively.
- The transformation properties of the GENERIC description facilitate the use of alternative thermodynamic variables such as the absolute temperature, the internal energy density, and the entropy density used in the present work.
- The newly proposed material form of the inelastic dissipative bracket (Section 3) makes possible to include into the GENERIC formulation often used nonlinear evolution laws for the internal variables associated with inelastic deformations.
- The mixed finite element discretization in space (Section 4) has been shown to be GENERIC-consistent. This means that the evolution equations for the state variables of the semi-discrete system fit into the GENERIC framework for discrete systems. This is an essential prerequisite for the development of fully structure-preserving EME schemes.

DATA AVAILABILITY STATEMENT
The data that support the findings of this study are available from the corresponding author upon reasonable request.

ORCID
Peter Betsch https://orcid.org/0000-0002-0596-2503

REFERENCES
1. Leimkuhler B, Reich S. *Simulating Hamiltonian Dynamics*. Vol 14. Cambridge, MA: Cambridge University Press; 2004.
2. Hairer E, Lubich C, Wanner G. *Geometric Numerical Integration*. Berlin, Germany: Springer Science & Business Media; 2006.
3. Marsden JE, Ratiu TS. *Introduction to Mechanics and Symmetry*. New York, NY: Springer; 1999.
4. Lew AJ, Marsden JE, Ortiz M, West M. An overview of variational integrators. *Finite Element Methods: 1970's and Beyond*. New York, NY: Springer; 2004:98-115.
5. Lall S, West M. Discrete variational Hamiltonian mechanics. *J Phys A Math Gen*. 2006;39(19):5509-5519.
6. LaBudde RA, Greenspan D. Energy and momentum conserving methods of arbitrary order for the numerical integration of equations of motion - I. motion of a Single of particles. *Numer Math*. 1976;25:323-346.
7. LaBudde RA, Greenspan D. Energy and momentum conserving methods of arbitrary order for the numerical integration of equations of motion - II. motion of a system of particles. *Numer Math*. 1976;26(4):1-16.
8. Gonzalez O. Exact energy-momentum conserving algorithms for general models in nonlinear elasticity. *Comput Methods Appl Mech Eng*. 2000;190(13-14):1763-1783.
9. Betsch P. *Structure-preserving Integrators in Nonlinear Structural Dynamics and Flexible Multibody Dynamics*. Vol 565. New York, NY: Springer; 2016.
10. Gebhardt C, Romero I, Rolfes R. A new conservative/dissipative time integration scheme for nonlinear mechanical systems. *Comput Mech*. 2020;65(2):405-427.
11. Mehrmann V, Morandin R. Structure-preserving discretization for port-Hamiltonian descriptor systems. Paper presented at: Proceedings of the 2019 IEEE 58th Conference on Decision and Control, Nice, France; 2019:6863-6868; IEEE.
12. Groß M, Betsch P. Energy-momentum consistent finite element discretization of dynamic finite viscoelasticity. *Int J Numer Methods Eng*. 2010;81(11):1341-1386.
13. Conde Martín S, García Orden JC, Romero I. Energy-consistent time integration for nonlinear viscoelasticity. *Comput Mech*. 2014;54(2):473-488.
14. Armero F, Zambrana-Rojas C. Volume-preserving energy-momentum schemes for isochoric multiplicative plasticity. *Comput Methods Appl Mech Eng*. 2007;196(41-44):4130-4159.

15. Groß M. *Higher-Order Accurate and Energy-Momentum Consistent Discretisation of Dynamic Finite Deformation Thermo-Viscoelasticity* [Habilitation thesis]. Universität Siegen; 2009.

16. Groß M, Bartelt M, Betsch P. Structure-preserving time integration of non-isothermal finite viscoelastic continua related to variational formulations of continuum dynamics. *Comput Mech*. 2018;62(2):123-150. http://dx.doi.org/10.1007/s00466-017-1489-x.

17. Groß M, Betsch P. Galerkin-based energy-momentum consistent time-stepping algorithms for classical nonlinear thermo-elastodynamics. *Math Comput Simul*. 2011;82(4):718-770.

18. Badlyan AM, Maschke BM, Beattie C, Mehrmann V. Open physical systems: from GENERIC to port-Hamiltonian systems; vol. 1, 2018:1-8. arXiv preprint arXiv:180404064.

19. Grmela M, Öttinger HC. Dynamics and thermodynamics of complex fluids. I. development of a general formalism. *Phys Rev E*. 1997;56(6):6620-6632.

20. Öttinger HC, Grmela M. Dynamics and thermodynamics of complex fluids. II. illustrations of a general formalism. *Phys Rev E*. 1997;56(6):6633-6655.

21. Öttinger HC. *Beyond Equilibrium Thermodynamics*. Hoboken, NJ: John Wiley & Sons; 2005.

22. Hütter M, Tervoort TA. Finite anisotropic elasticity and material frame indifference from a non-equilibrium thermodynamics perspective. *J Non-Newtonian Fluid Mech*. 2008;152(1-3):45-52.

23. Hütter M, Svendsen B. On the formulation of continuum thermodynamic models for solids as general equations for non-equilibrium reversible-irreversible coupling. *J Elast*. 2011;104:357-368.

24. Hütter M, Svendsen B. Thermodynamic model formulation for viscoplastic solids as general equations for non-equilibrium reversible-irreversible coupling. *Contin Mech Thermodyn*. 2012;24(3):211-227.

25. Mielke A. Formulation of thermoelastic dissipative material behavior using GENERIC. *Contin Mech Thermodyn*. 2011;23(3):233-256.

26. Romero I. Thermodynamically consistent time-stepping algorithms for non-linear thermomechanical systems. *Int J Numer Methods Eng*. 2009;79(6):706-732.

27. Simo JC, Tarnow N. The discrete energy-momentum method conserving algorithms for nonlinear elastodynamics. *J Appl Math Phys*. 1992;43(5):757-792.

28. Betsch P, Steinmann P. Conservation properties of a time FE method––Part II: time-stepping schemes for non-linear elastodynamics. *Int J Numer Methods Eng*. 2001;50:1931-1955.

29. Krüger M, Groß M, Betsch P. An energy-entropy-consistent time stepping scheme for nonlinear thermo-viscoelastic continua. *ZAMM-J Appl Math Mech/Zeitschrift für Angewandte Mathematik und Mechanik*. 2016;96(2):141-178.

30. Romero I. Algorithms for coupled problems that preserve symmetries and the laws of thermodynamics. Part I: monolithic integrators and their application to finite strain thermoelasticity. *Comput Methods Appl Mech Eng*. 2010;199(25-28):1841-1858.

31. Romero I. Algorithms for coupled problems that preserve symmetries and the laws of thermodynamics. Part II: fractional step methods. *Comput Methods Appl Mech Eng*. 2010;199(33-36):2235-2248.

32. García Orden JC, Romero I. Energy-entropy-momentum integration of discrete thermo-visco-elastic dynamics. *Europ J Mech A/Solids*. 2012;32:76-87.

33. Conde Martín S, Betsch P, García Orden JC. A temperature-based thermodynamically consistent integration scheme for discrete thermo-elastodynamics. *Commun Nonlinear Sci Numer Simul*. 2016;32:63-80.

34. Conde Martín S. *Energy-Entropy-Momentum Time Integration Methods for Coupled Smooth Dissipative Problems* [PhD dissertation]. Universidad Politécnica de Madrid (UPM); 2016.

35. Portillo D, García Orden JC, Romero I. Energy–entropy–momentum integration schemes for general discrete non-smooth dissipative problems in thermomechanics. *Int J Numer Methods Eng*. 2017;112(7):776-802.

36. Conde Martín S, García Orden J. On energy-entropy-momentum integration methods for discrete thermo-visco-elastodynamics. *Comput Struct*. 2017;181:3-20.

37. Öttinger HC. GENERIC integrators: structure preserving time integration for thermodynamic systems. *J Non-Equil Thermody*. 2018;43(2):89-100.

38. Shang X, Öttinger HC. Structure-preserving integrators for dissipative systems based on reversible-irreversible splitting royalsocietypublishingorg. *Proc Royal Soc A*. 2020;476(2234).

39. Betsch P, Schiebl M. GENERIC-based formulation and discretization of initial boundary value problems for finite strain thermoelasticity. *Comput Mech*. 2020;65(2):503-531.

40. Betsch P, Schiebl M. Energy-momentum-entropy consistent numerical methods for large-strain thermoelasticity relying on the GENERIC formalism. *Int J Numer Methods Eng*. 2019;119(12):1216-1244.

41. Gonzalez O. Time integration and discrete Hamiltonian systems. *J Nonlinear Sci*. 1996;6(5):449-467.

42. Gonzalez O, Stuart AA. *First Course in Continuum Mechanics*. Cambridge, MA: Cambridge University Press; 2008.

43. Reese S, Govindjee S. A theory of finite viscoelasticity and numerical aspects. *Int J Solids Struct*. 1998;35(26-27):3455-3482.

44. Sidoroff F. Nonlinear viscoelastic model with intermediate configuration. *J Mecanique*. 1974;13(4):679-713.

45. Reese S, Govindjee S. Theoretical and numerical aspects in the thermo-viscoelastic material behaviour of rubber-like polymers. *Mech Time Depend Mater*. 1998;1(4):357-396.

46. Budday S, Ovaert TC, Holzapfel GA, Steinmann P, Kuhl E. *Fifty Shades of Brain: A Review on the Mechanical Testing and Modeling of Brain Tissue*. Vol 27. Amsterdam, Netherlands: Springer; 2019.

47. Hughes TJ. *The Finite Element Method: Linear Static and Dynamic Finite Element Analysis*. New York, NY: Courier Corporation; 2003.

48. Gurtin ME. Thermodynamics and stability. *Arch Ration Mech Anal*. 1975;59(1):63-96.

49. Hartmann S. A remark on the application of the Newton-Raphson method in non-linear finite element analysis. *Comput Mech.* 2005;36(2):100-116.

50. Netz T, Hartmann S. A monolithic finite element approach using high-order schemes in time and space applied to finite strain thermo-viscoelasticity. *Comput Math Appl.* 2015;70(7):1457-1480.

51. Schröder J, Lion A, Johlitz M. *On the Derivation and Application of a Finite Strain Thermo-Viscoelastic Material Model for Rubber Components.* Cham, Switzerland: Springer International Publishing; 2019:325-348.

APPENDIX A. ROTATIONAL SYMMETRY

Due to invariance under superposed rigid rotations, the present problem satisfies symmetry properties (93). To see this, we consider a rotation tensor $\mathbf{Q}^\varepsilon = \exp(\varepsilon\widehat{\boldsymbol{\xi}})$, expressed through the Rodrigues formula.[3] Here, ε is a scalar parameter and $\widehat{\boldsymbol{\xi}}$ is a skew-symmetric tensor with associated vector $\boldsymbol{\xi} \in \mathbb{R}^3$, such that $\widehat{\boldsymbol{\xi}}\mathbf{a} = \boldsymbol{\xi} \times \mathbf{a}$ for all $\mathbf{a} \in \mathbb{R}^3$. Now, a superposed rigid motion gives rise to rotated nodal position vectors

$$\mathbf{q}_a^\varepsilon = \mathbf{Q}^\varepsilon \mathbf{q}_a. \tag{A1}$$

Note that $\mathbf{q}_a^0 = \mathbf{q}_a$ and $\left.\frac{d}{d\varepsilon}\mathbf{Q}^\varepsilon\right|_{\varepsilon=0} = \widehat{\boldsymbol{\xi}}$. Nodal pattern (A1) of the rigidly rotated discrete system gives rise to the corresponding expression for the discrete deformation gradient (cf. (53)$_1$)

$$\mathbf{F}^{\mathrm{h},\varepsilon} = \mathbf{q}_a^\varepsilon \otimes \nabla N^a = \mathbf{Q}^\varepsilon \mathbf{F}^{\mathrm{h}}. \tag{A2}$$

Furthermore, the corresponding right Cauchy-Green deformation tensor follows from (3) and is given by

$$\mathbf{C}^{\mathrm{h},\varepsilon} = (\mathbf{F}^{\mathrm{h},\varepsilon\mathrm{T}})\mathbf{F}^{\mathrm{h},\varepsilon} = \mathbf{C}^{\mathrm{h}}, \tag{A3}$$

where property $(\mathbf{Q}^\varepsilon)^{\mathrm{T}} = (\mathbf{Q}^\varepsilon)^{-1}$ of the rotation tensor has been taken into account. A frame-indifferent formulation implies that the internal energy density takes the form $u(\mathbf{F}, \tau, \mathbf{C}_p^{-1}) = u(\mathbf{C}, \tau, \mathbf{C}_p^{-1})$. Thus, taking the derivative of $u(\mathbf{F}^{\mathrm{h},\varepsilon}, \tau, \mathbf{C}_p^{-1}) = u(\mathbf{C}^h, \tau, \mathbf{C}_p^{-1})$ with respect to parameter ε and subsequently setting $\varepsilon = 0$ yields

$$\begin{aligned}
0 &= \left.\frac{d}{d\varepsilon}\right|_{\varepsilon=0} u\left(\mathbf{F}_g^{\mathrm{h},\varepsilon}, \tau_g^{\mathrm{h}}, (\mathbf{C}_p^{-1})_g\right) \\
&= \partial_{\mathbf{F}} u_g : \left.\frac{d}{d\varepsilon}\right|_{\varepsilon=0} \mathbf{q}_a^\varepsilon \otimes \nabla N_g^a \\
&= \partial_{\mathbf{F}} u_g : \left(\widehat{\boldsymbol{\xi}}\mathbf{q}_a \otimes \nabla N_g^a\right) \\
&= (\boldsymbol{\xi} \times \mathbf{q}_a) \cdot \partial_{\mathbf{F}} u_g \nabla N_g^a \\
&= \boldsymbol{\xi} \cdot \left(\mathbf{q}_a \times \partial_{\mathbf{F}} u_g \nabla N_g^a\right),
\end{aligned} \tag{A4}$$

where u_g is given by (52)$_1$. Due to the arbitrariness of $\boldsymbol{\xi} \in \mathbb{R}^3$ (and vanishing body forces), the last equation coincides with symmetry condition (93)$_1$, that is

$$\mathbf{q}_a \times \partial_{\mathbf{q}_a}\mathcal{E} = \mathbf{0}.$$

Note that this condition holds as well for the specific choice $\tau = u$, due to (97)$_1$.

Similarly, symmetry condition (93)$_2$ results from the frame-indifference of the entropy density function $\eta(\mathbf{F}, \tau, \mathbf{C}_p^{-1}) = \eta(\mathbf{C}, \tau, \mathbf{C}_p^{-1})$, or from (100)$_1$ in the case $\tau = \eta$.

APPENDIX B. DISCRETE DERIVATIVES

This appendix provides the specific definitions of the discrete derivatives $d_{\mathbf{C}}u$, $d_{\tau}u$, and $du/d(\mathbf{C}_p^{-1})$. To this end, we resort to the notion of "partitioned discrete derivative" introduced in Gonzalez.[41] Accordingly, with regard to the internal energy density $u(\mathbf{C}, \tau, \mathbf{C}_p^{-1})$, we introduce the discrete derivative

$$d_{\mathbf{C}}u = \frac{1}{2}\left(D_{\mathbf{C}}u(\bullet, \tau_{n+1}, \mathbf{C}_{p_{n+1}}^{-1}) + D_{\mathbf{C}}u(\bullet, \tau_n, \mathbf{C}_{p_n}^{-1})\right), \tag{B1}$$

where

$$D_{\mathbf{C}}u(\bullet, \tau, \mathbf{C}_p^{-1}) = \partial_{\mathbf{C}}u(\mathbf{C}_{n+\frac{1}{2}}, \tau, \mathbf{C}_p^{-1})$$
$$+ \frac{u(\mathbf{C}_{n+1}, \tau, \mathbf{C}_p^{-1}) - u(\mathbf{C}_n, \tau, \mathbf{C}_p^{-1}) - \partial_{\mathbf{C}}u(\mathbf{C}_{n+\frac{1}{2}}, \tau, \mathbf{C}_p^{-1}) : \Delta\mathbf{C}}{\Delta\mathbf{C} : \Delta\mathbf{C}}\Delta\mathbf{C}.$$

Here, $\Delta\mathbf{C} = \mathbf{C}_{n+1} - \mathbf{C}_n$. Furthermore, we have

$$d_{\tau}u = \frac{1}{2}\left(D_{\tau}u(\mathbf{C}_n, \bullet, \mathbf{C}_{p_{n+1}}^{-1}) + D_{\tau}u(\mathbf{C}_{n+1}, \bullet, \mathbf{C}_{p_n}^{-1})\right), \tag{B2}$$

where

$$D_{\tau}u(\mathbf{C}, \bullet, \mathbf{C}_p^{-1}) = \frac{u(\mathbf{C}, \tau_{n+1}, \mathbf{C}_p^{-1}) - u(\mathbf{C}, \tau_n, \mathbf{C}_p^{-1})}{\Delta\tau},$$

and $\Delta\tau = \tau_{n+1} - \tau_n$. Eventually,

$$\frac{du}{d\mathbf{C}_p^{-1}} = \frac{1}{2}\left(D_{\mathbf{C}_p^{-1}}u(\mathbf{C}_{n+1}, \tau_{n+1}, \bullet) + D_{\mathbf{C}_p^{-1}}u(\mathbf{C}_n, \tau_n, \bullet)\right), \tag{B3}$$

where

$$D_{\mathbf{C}_p^{-1}}u(\mathbf{C}, \tau, \bullet) = \partial_{\mathbf{C}_p^{-1}}u(\mathbf{C}, \tau, \mathbf{C}_{p_{n+\frac{1}{2}}}^{-1})$$
$$+ \frac{u(\mathbf{C}, \tau, \mathbf{C}_{p_{n+1}}^{-1}) - u(\mathbf{C}, \tau, \mathbf{C}_{p_n}^{-1}) - \partial_{\mathbf{C}_p^{-1}}u(\mathbf{C}, \tau, \mathbf{C}_{p_{n+\frac{1}{2}}}^{-1}) : \Delta\mathbf{C}_p^{-1}}{\Delta\mathbf{C}_p^{-1} : \Delta\mathbf{C}_p^{-1}}\Delta\mathbf{C}_p^{-1},$$

and $\Delta\mathbf{C}_p^{-1} = \mathbf{C}_{p_{n+1}}^{-1} - \mathbf{C}_{p_n}^{-1}$. Analogous expressions are used for the discrete derivatives of the entropy density $\eta(\mathbf{C}, \tau, \mathbf{C}_p^{-1})$. Note that the above expressions for the discrete derivatives are typically evaluated in the integration points $g \in \{1, \ldots, G\}$.

Next, we verify directionality property $(118)_1$. For that purpose, we make use of the discrete derivatives of the total energy introduced in (111), to obtain

$$d\mathcal{E}(\mathbf{z}_n, \mathbf{z}_{n+1}) \cdot (\mathbf{z}_{n+1} - \mathbf{z}_n)$$
$$= d_{\mathbf{q}_a}\mathcal{E} \cdot \left(\mathbf{q}_{a_{n+1}} - \mathbf{q}_{a_n}\right) + d_{\mathbf{p}^a}\mathcal{E} \cdot \left(\mathbf{p}_{n+1}^a - \mathbf{p}_n^a\right)$$
$$+ d_{\tau_a}\mathcal{E}\left(\tau_{a_{n+1}} - \tau_{a_n}\right) + \sum_{g=1}^{G}\frac{d\mathcal{E}}{d(\mathbf{C}_p^{-1})_g^{AB}}\left((\mathbf{C}_p^{-1})_{g_{n+1}}^{AB} - (\mathbf{C}_p^{-1})_{g_n}^{AB}\right)$$
$$= \sum_{g=1}^{G}w_g\left(2\mathbf{F}_{g_{n+\frac{1}{2}}}d_{\mathbf{C}}u_g\nabla N_g^a\right)\cdot\left(\mathbf{q}_{a_{n+1}} - \mathbf{q}_{a_n}\right) + M_{ab}\mathbf{p}_{n+\frac{1}{2}}^b\cdot\left(\mathbf{p}_{n+1}^a - \mathbf{p}_n^a\right)$$
$$+ \sum_{g=1}^{G}w_g N_g^a d_{\tau}u_g\left(\tau_{a_{n+1}} - \tau_{a_n}\right) + \sum_{g=1}^{G}w_g\frac{du_g}{d\mathbf{C}_p^{-1}} : \left((\mathbf{C}_p^{-1})_{g_{n+1}} - (\mathbf{C}_p^{-1})_{g_n}\right)$$

$$= \sum_{g=1}^{G} w_g \mathrm{d}_{\mathbf{C}} u_g \; : \; \left(\mathbf{C}_{g_{n+1}}^{\mathrm{h}} - \mathbf{C}_{g_n}^{\mathrm{h}} \right) + \mathcal{T}_{n+1} - \mathcal{T}_n$$

$$+ \sum_{g=1}^{G} w_g \mathrm{d}_\tau u_g \left(\tau_{g_{n+1}}^{\mathrm{h}} - \tau_{g_n}^{\mathrm{h}} \right) + \sum_{g=1}^{G} w_g \frac{\mathrm{d} u_g}{\mathrm{d} \mathbf{C}_p^{-1}} \; : \; \left((\mathbf{C}_p^{-1})_{g_{n+1}} - (\mathbf{C}_p^{-1})_{g_n} \right).$$

Note that, for simplicity, body forces have been neglected in the above equations. Moreover, the total kinetic energy of the semi-discrete system at time t_n is given by

$$\mathcal{T}_n = \frac{1}{2} M_{ab} \mathbf{p}_n^a \cdot \mathbf{p}_n^b.$$

Now, making use of expressions (B1), (B2), and (B3), for the discrete derivatives $\mathrm{d}_{\mathbf{C}} u$, $\mathrm{d}_\tau u$, and $\mathrm{d} u / \mathrm{d}(\mathbf{C}_p^{-1})$, respectively, it can be shown by a straightforward calculation that

$$\mathrm{d}_{\mathbf{C}} u_g \; : \; \left(\mathbf{C}_{g_{n+1}}^{\mathrm{h}} - \mathbf{C}_{g_n}^{\mathrm{h}} \right) + \mathrm{d}_\tau u_g \left(\tau_{g_{n+1}}^{\mathrm{h}} - \tau_{g_n}^{\mathrm{h}} \right) + \frac{\mathrm{d} u_g}{\mathrm{d} \mathbf{C}_p^{-1}} \; : \; \left((\mathbf{C}_p^{-1})_{g_{n+1}} - (\mathbf{C}_p^{-1})_{g_n} \right)$$

$$= u_{g_{n+1}} - u_{g_n}.$$

Note that expression u_g has been introduced in (52). Correspondingly, u_{g_n} stands for the internal energy density at point $\mathbf{X}_g$ and time t_n. That is, $u_{g_n} = u\left(\mathbf{C}_{g_n}^{\mathrm{h}}, \tau_{g_n}^{\mathrm{h}}, (\mathbf{C}_p^{-1})_{g_n} \right)$. Upon introduction of the total internal energy of the semi-discrete system at time t_n,

$$\mathcal{U}_n = \sum_{g=1}^{G} w_g u_{g_n},$$

we eventually obtain the result

$$\mathrm{d}\mathcal{E}(\mathbf{z}_n, \mathbf{z}_{n+1}) \cdot (\mathbf{z}_{n+1} - \mathbf{z}_n) = \mathcal{E}_{n+1} - \mathcal{E}_n,$$

where the total energy of the semi-discrete system at time t_n is given by

$$\mathcal{E}_n = \mathcal{U}_n + \mathcal{T}_n.$$

The validity of the second directionality property $(118)_2$ can be shown in an analogous way.